lubricants

MDPI

Article

Impact of Temperature Variation on Friction Behaviour of Rare Earth-Doped Diamond-like Carbon Coatings with Ionic Liquid Lubricants

Shahsharif Shaikh [1], Takeru Omiya [1,2,*], Albano Cavaleiro [1,2], Luis Vilhena [1], Amilcar Ramalho [1] and Fábio Ferreira [1,2,3]

[1] CEMMPRE Centre for Mechanical Engineering Materials and Processes, Department of Mechanical Engineering, University of Coimbra, Rua Luís Reis Santos, 3030-788 Coimbra, Portugal; shaikhshahsharif@gmail.com (S.S.); albano.cavaleiro@dem.uc.pt (A.C.); luis.vilhena@uc.pt (L.V.); amilcar.ramalho@dem.uc.pt (A.R.); fabio.ferreira@dem.uc.pt (F.F.)
[2] Laboratory for Wear, Testing and Materials, Instituto Pedro Nunes, Rua Pedro Nunes, 3030-199 Coimbra, Portugal
[3] Walker Department of Mechanical Engineering, The University of Texas at Austin, Austin, TX 78712, USA
* Correspondence: takeru.omiya@student.dem.uc.pt

Abstract: This research paper investigates the tribological performance of diamond-like carbon (DLC) coatings doped with rare earth metals (europium and gadolinium) as well as pure DLC lubricated with ionic liquid additives (trihexyltetradecylphosphonium bis(2-ethylhexyl) phosphate {[P_{66614}][DEHP]} and 1-ethyl-3-methylimidazolium diethyl phosphate {[EMIM][DEP]}) in Polyalphaolefin 8 (PAO8). The study aims to examine the effect of temperature on the interaction between the coatings and additives by conducting tribological experiments using a block-on-disk setup at temperatures of 60 °C, 80 °C, and 100 °C. The primary objective is to evaluate the performance of doped DLC coatings compared to pure DLC coatings with ionic liquid additives in the lubricant in boundary lubrication conditions at various high working temperature environments. The experiments reveal that doped DLC coatings with ionic liquid additives exhibit superior tribological performance compared to pure DLC coatings. The rare earth metal dopants play a positive role in the formation of a tribofilm on the surface of the coatings as it interacts with ionic liquids, resulting in a lower coefficient of friction (CoF). Temperature influences the performance of the coatings and additives. The CoF increases with temperature for pure DLC coatings, while for doped DLC coatings it was significantly less. These findings highlight the influence of temperature on the tribological behavior of DLC coatings. Overall, this study contributes valuable insights into the impact of rare earth metal dopants and ionic liquid additives on the tribological performance of DLC coatings under different temperature conditions. The results demonstrate the potential of utilizing doped DLC coatings with ionic liquid additives as an effective approach to enhance the performance of mechanical systems.

Keywords: ionic liquids; diamond-like carbon coatings; doped-DLC; tribology; temperature

Citation: Shaikh, S.; Omiya, T.; Cavaleiro, A.; Vilhena, L.; Ramalho, A.; Ferreira, F. Impact of Temperature Variation on Friction Behaviour of Rare Earth-Doped Diamond-like Carbon Coatings with Ionic Liquid Lubricants. *Lubricants* **2023**, *11*, 302. https://doi.org/10.3390/lubricants11070302

Received: 14 June 2023
Revised: 12 July 2023
Accepted: 17 July 2023
Published: 20 July 2023

1. Introduction

Climate change has raised concerns about the impact of fossil fuels on the environment, leading to a search for sustainable alternatives [1]. Frictional losses account for a significant portion of energy wastage, with around one-third of total energy production lost to friction, wear, and tear of components [2]. Reduction of frictional losses can result in decreased energy consumption, increased productivity, and monetary savings. Diamond-Like-Carbon (DLC) coatings, known for their superior tribological and mechanical properties, such as high wear resistance, hardness, and low coefficient of friction (CoF), have emerged as a promising solution [3–5].

DLC coatings are a type of self-lubricating coatings [6–9]. These coatings can be classified as diamond-like carbon (DLC) or graphite-like carbon (GLC) from the carbon fractions of sp^2 and sp^3 in coatings. DLC coatings predominantly contain the sp^3 carbon fraction, while graphite-like carbon coatings have a dominant sp^2 fraction [10]. DLC coatings are governed by ISO 20523:2017 which was established by the International Organization for Standardization (ISO) to provide guidelines for classifying, designating, and naming carbon-based films. These films may contain other elements such as hydrogen or metals. Metal carbides can be included as constituents in the films. ISO 20523:2017 only applies to films where carbon is the main component if additional elements are present [11].

The push to minimize the use of lubricants in mechanical systems poses a challenge for engineers to operate under boundary lubrication conditions. DLC coatings have been found to exhibit the lowest CoF, and their chemical structure can be tuned for various industrial applications [12–15]. However, pure DLC coatings are inert and do not react with conventional lubricants to form a protective tribofilm, leading to wear and tear [14]. Conventional lubricants are not sustainable and may not perform well with DLC coatings. Ionic liquids (ILs) have emerged as a promising solution due to their high thermal stability, low vapor pressure, low flammability, and tuneable properties for specific applications [16–21]. Phosphorus-based ionic liquids, in particular, have shown promising results in reducing friction under boundary lubrication conditions by forming a tribofilm [22–24]. ILs are liquid salts composed of organic substances, characterized by a low melting temperature, high combustible temperature, low vapor pressure, superior thermal stability, low volatility, and high miscibility with organic substances [25]. They offer several advantages in lubrication systems, including reduced energy consumption, protection against friction and wear, and improved longevity [25–29]. ILs can be tailor-made to meet specific requirements by varying the combination of cations and anions [30].

The cationic structure of ILs contributes to their exceptional properties, such as high miscibility with lubricants, low melting point, superior thermal stability, and unique molecular structure [31]. The spherical shape of the ions and the variations in alkyl chains and quadrilateral structures enhance the lubrication properties of ILs, making them suitable for high-performance lubricants [32]. The anionic structure of ILs, such as hexafluorophosphate (PF_6) and tetrafluoroborate (BF_4), contributes to the formation of protective films that improve the wear resistance of the lubricated surfaces [23,33–37]. The tribological efficiency of ILs depends on the nature of the anion and cation, with phosphonium-based ILs exhibiting higher tribological properties. Hydrophobic ILs generally perform better in tribological applications compared to hydrophilic ILs [38].

ILs have demonstrated remarkable tribological behavior as both neat lubricants and additives [39]. They can form lubrication films on interacting surfaces, resulting in reduced friction and wear. ILs have been investigated for their potential to enhance the tribological properties of traditional lubricant systems as additives [40]. The electrical charge of the DLC surface and the adsorption ability of the lubricant played significant roles in friction control [41,42]. The electrical conductivity of the lubricant (ionic liquid) affected the transport of additives to the surface, ultimately impacting friction. Higher electrical conductivity in IL-additivated lubricants resulted in faster transport kinetics and lower friction [43].

Overall, the combination of doped DLC coatings and ILs showed promising results in improving tribological properties. The addition of doping elements enhanced the performance of DLC coatings, while ILs with their lubricity and thermal stability proved to be suitable for various tribological applications. The combination of doped DLC coatings and ILs was reported to further enhance their tribological properties through the formation of a protective film or tribofilm on the coating surface.

In this study, we will be using trihexyltetradecylphosphonium bis(2-ethylhexyl) phosphate [P_{66614}] [DEHP], which has been shown to react with iron surfaces and form an iron phosphate tribofilm layer [44–46]. In situ atomic force microscopy (AFM) by Li et al. has confirmed the adsorption of [P_{66614}] [DEHP] on the iron surface through its phosphate anions, resulting in reduced nanoscale friction [47]. Another ionic liquid lubricant additive,

1-Ethyl-3-methylimidazolium diethylphosphate ([EMIM][DEP]), has shown low wear rate and CoF due to its phosphorus-based anions [48–52]. DEP has also been recognized as a green and sustainable solvent for a sustainable future [53–55]. The phenomenon of chemical wear, resulting in reduced CoF and increased wear volume, has been observed with DEP [52]. The ionic liquid additives in PAO8 will henceforth be reported as either Ionic Liquid #1 or IL#1 for PAO 8 + 1 wt.% {[P_{66614}][DEHP]} and Ionic Liquid #2 or IL#2 for PAO 8 + 1 wt.% {[EMIM][DEP]}.

DLC thin films may wear out quickly in dry conditions, despite being called self-lubricating coatings. To make them last longer, a liquid lubricant can be used [56]. DLC coatings have a drawback: they don't react well with the oil additives currently used, which means that protective films that reduce wear are not easily formed. Many studies have been conducted on the interaction between base oils, lubricant additives, and doped DLC coatings over the past 30 years, but there is no consensus yet, moreover there is little to no research on the interaction of doped DLC and ionic liquids [57–62]. To overcome this limitation, doping with metals such as tungsten, zirconium, titanium, chromium, and silver has been done and it is successful in improving their thermal stability, corrosion resistance, and adhesion to the substrate, but the coefficient of friction still remains comparatively high [63–71]. Additionally, the lubrication mechanism and performance of new additives, developed to improve energy efficiency in moving mechanical components, when used with DLC films, are still un-known. The researchers have explored the tribological behavior of DLC coatings doped with rare earth metals like Gd and Eu, which showed significant improvement in the reaction with ionic liquids and doped DLC [72]. Research done by Omiya et.al. and Sadeghi et.al has shown that as the concentration of dopants (Eu and Gd) increases in the DLC, their affinity towards the ionic liquid additivated lubricant increases [73,74].

Despite the importance of these studies, only a few have focused on the benefits of using DLCs lubricated by ILs (ionic liquids) as a lubricant or oils that contain ILs with anti-wear additives. Therefore, for our experimental investigation, we will be employing Europium and Gadolinium as dopants of rare earth elements in DLC coatings to study their interaction with ionic liquids as additives in Polyalphaolefin 8 (PAO8). The rare earth elements are unexplored in the field of doping of DLC. Ionic liquids have been in use as solvent for the extraction of Europium and Gadolinium due to their affinity towards them [75]. Prior research has shown that ionic liquids can enhance the luminescence properties of rare earth metals and are used in their extraction processes [76–79]. The trivalent oxidation state of lanthanide ions makes them attractive for tribological processes with ionic liquids and their impact on tribolayer formation will be investigated. The tribological processes, where ILs serve as anti-wear additives, are expected to be influenced using lanthanides, according to these indications. Non rare earth metals have been used in doping and they have improved their thermal stability, corrosion resistance, and adhesion to the substrate, but the coefficient of friction still remains comparatively high or there are some caveats. Khanmohammadi et.al did experiments by doping DLC with silver which improved the properties, but CoF was high, whereas tungsten dopant showed good results but was limited to low temperature with glycol based water lubricant [43]. In another study, researchers conducted a study on Cr-doped coatings made of diamond-like carbon (Cr-DLC) using PVD and PECVD methods [80]. The lubrication performance of solid-liquid composite lubrication systems was studied using two ionic liquids (ILs) as lubricants. The findings indicated that the friction coefficient was reduced but it corroded the surface [80].

Therefore, to assess the tribological performance, a comprehensive study was conducted by us to examine the behavior of lanthanides, specifically gadolinium (Gd) and europium (Eu), as reactive elements on the surface of diamond-like carbon (DLC) coatings. The DLC coatings were prepared using a deposition technique known as High Power Impulse Magnetron Sputtering (HiPIMS). The objective was to evaluate the lubrication effectiveness of these coatings when subjected to sliding against steel surfaces, in the presence of lubricants with ILs as additives compared to regularly used base oil (BO). Comparing

the samples lubricated with ILs and base oil along with various temperatures has allowed for a comprehensive evaluation of the dependency of ILs and the efficacy of the doping process on enhancing the lubrication performance of ILs in tribological applications.

2. Materials and Methods

2.1. Specimens

There is a total of three DLC coatings which are selected, namely 2.3% Gd-DLC, 2.4% Eu-DLC and pure DLC as a reference. The study utilizes steel substrates (AISI D2) that are 25 mm in diameter and 8 mm thick. The substrates are first mirror polished with an Ra < 0.05 µm and then the DLC films are deposited on them. Subsequently, the samples are cleaned by placing them in an ultrasonic bath filled with acetone and ethanol for 15 to 20 min.

After cleaning, the D2 samples are attached to an aluminum holder using silver glue and placed in the deposition chamber. The DLC coatings are deposited using the sputtering method with a DOMS power supply and a pure graphite target. Pellets containing Europium and Gadolinium are used in the target to achieve the desired composition. The chamber is then vacuumed and maintained at a pressure of 3×10^{-4} Pa using a turbomolecular pump. Before depositing the DLC coatings, the substrate and target are cleaned to remove any surface oxides for 10 minutes using a power supply of 600 W at a pressure of 0.4 Pa. Next, a Chromium interlayer is deposited to enhance adhesion on the substrate using direct-current magnetron sputtering. A 400 nm thick CrN layer is then deposited with an Ar:N_2 gas flow ratio of 1:3 for 7 minutes at 0.3 Pa.

Finally, the DLC coatings are deposited by HiPIMS for a duration of 57 minutes under a pressure of 0.4 Pa. This process results in the formation of the desired DLC coatings on the steel substrates, which can be further analyzed and characterized for their properties and performance in the study. The wear rate of the coatings can be enhanced by the specific type and quantity of doped metals, thereby implying that the ionic liquid (IL) has the potential to improve their wear resistance characteristics [73]. Furthermore, it was observed by Omiya et. al. that an increase in the atomic concentration of the doped metal led to a greater reduction in friction, particularly in Gd-doped diamond-like carbon (DLC) coatings compared to Eu-doped DLC coatings [73].

The HiPIMS deposition technique was used to coat the samples, and the aspect of the DLCs coatings is shown in Figure 1. Carbon clusters or a cauliflower-like structure can be observed in all three samples, which is a common characteristic of DLCs coatings. These clusters do not represent the actual grain structure, but rather the carbon-amorphous regions [81–85]. It is evident that the size and shape of the carbon clusters depend on the deposition technique. Additionally, these regions with a high carbon content indicate the density of the film. Therefore, a denser film is achieved when the carbon clusters are smaller [86–88]. Consequently, all three samples (2.3% Gd-DLC; 2.4% Eu-DLC; and Pure DLC) exhibit a similar structure and thickness, indicating the uniform coating achieved through our HiPIMS process.

To examine the detailed morphology of the coating's cross-section, SEM was used with a magnification of 25kX and a spot size of 75pA which can be seen in Figure 2. The cross-sectional view revealed columnar and porous structures. At the top of these columnar structures, there are dome-shaped bumps resembling hats, which indicate the morphology of the cross-section. The adhesion between the substrate and the coating is improved by a chromium interlayer, which forms a compact structure. The thickness of all the coatings is similar, with the total film and interlayer thicknesses measuring approximately (1.7 ± 0.1) µm and (0.45 ± 0.05) µm, respectively, based on the measurement scale.

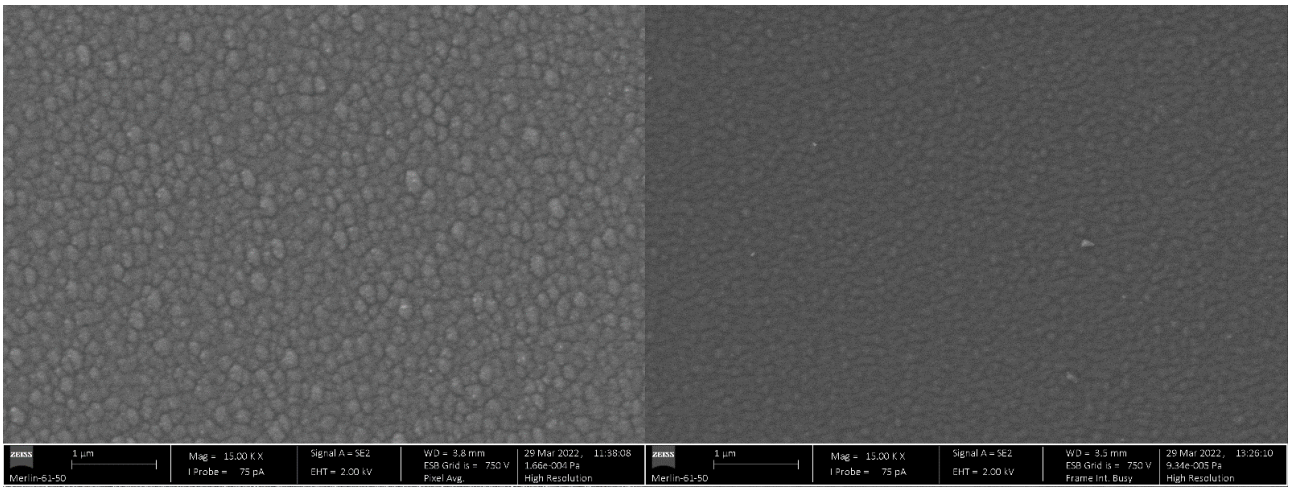

Figure 1. Examination of DLC coating structure under SEM.: (**a**) 2.3% Gd-DLC; (**b**) 2.4% Eu-DLC; (**c**) Pure DLC.

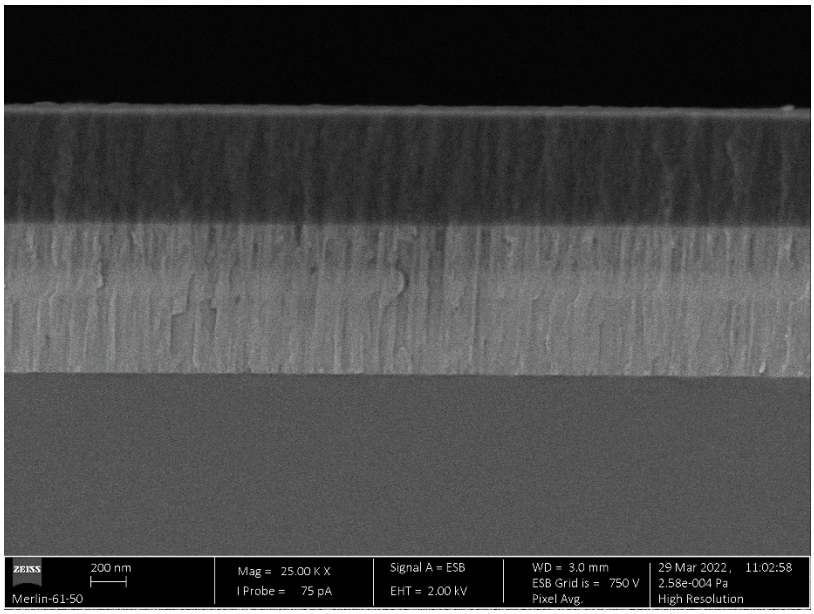

Figure 2. Examination of cross-sectional morphology of DLC coating under SEM.

2.2. Lubricants

The base lubricant used was PAO8. Synthesis of trihexyltetradecylphosphonium bis(2-ethylhexyl) phosphate [P_{66614}][DEHP] was conducted according to the procedure described in [18]. In brief, trihexyl(tetradecyl)phosphonium bromide (with a purity of 95%, obtained from Strem chemicals) was combined with methanol and treated with Amberlite IRN78 (with a purity of 99.9%, obtained from Alfa Aesar) to obtain trihexyl(tetradecyl)phosphonium hydroxide. The resulting mixture was then filtered and subjected to a 3-day reaction with bis(2-ethylhexyl) hydrogen phosphate (obtained from TCI). Methanol and other volatile compounds were subsequently removed under reduced pressure (approximately 8 Torr) and at a temperature of around -50 °C. The water content in the as-synthesized [P_{66614}][DEHP] was determined to be 0.07 % (equivalent to 700 ppm). The estimated purity of the as-synthesized [P_{66614}][DEHP] was ≥92 % based on nuclear magnetic resonance (NMR) spectroscopy analysis. To prepare the lubricant containing PAO 8 and 1 wt.% of [P_{66614}][DEHP], 1 g of [P_{66614}][DEHP] was mixed with 99 g of PAO8 using an analytical balance [73].

2.3. Tribological Tests

The three DLC coated specimens undergo testing utilizing a block-on-ring configuration tribometer, under unidirectional sliding motion. The stationary block, consisting of the DLC coated specimens, is subjected to a constant applied load during the test and pressed against a rotating ring. The rotating ring is constructed of alloyed carbon steel (3415, AISI) with a hardness of 237 HV_{10} (kgf/mm^2) and has a dimension of Ø ≥ 150 × 12 mm. The rotating ring is positioned at a 90° angle relative to its axis of rotation and has an initial surface roughness of Ra = 0.01 µm. A schematic diagram of the block-on-ring configuration can be seen in Figure 3.

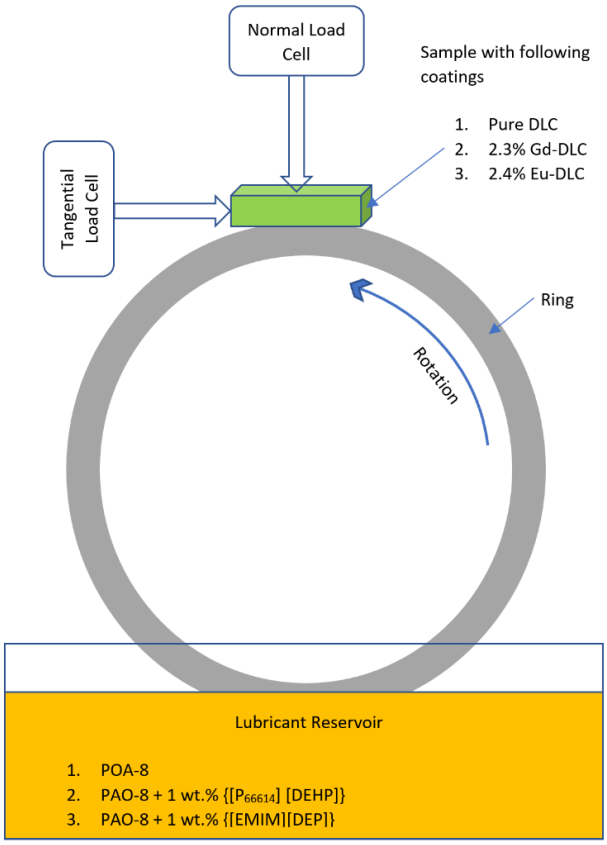

Figure 3. Schematic diagram of block-on-ring friction tribometer.

The normal applied load and friction force between the block and the ring were continuously monitored throughout the testing process using two load cells, which facilitated real-time computation of the friction coefficient. A normal load of 25 N was applied during the test. The normal force load cell served as the input for normal force (F_N) and a tangential force load cell measured the friction force (F_f). The coefficient of friction (μ) was calculated by dividing F_f by F_N. A lubricant reservoir was utilized to keep the contact lubricated with lubricating oil. A radiation heating system was utilized for temperature control during the tests, enabling the execution of tests at various high temperatures in oil, which were 60 °C, 80 °C, and 100 °C in the study. The test setup can be seen in Figure 4.

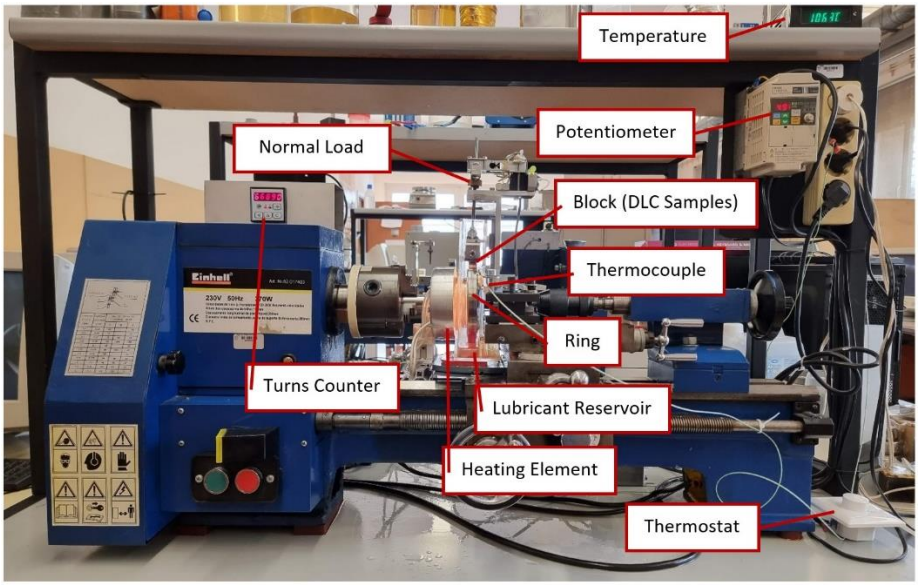

Figure 4. Block on ring test setup with all instruments.

During tribological testing, three different lubricants were utilized, which were established as fully flooded with a homogenous film of lubricant that wetted the contact region. The rotation of the ring within the lubricant, created a constant and uniform film of several millimeters in thickness on the surface of the ring, with the oil being picked up by the rotating disk and supplied to the contact before flowing back to the lubricant housing. The tribometer utilized in this study, which is particularly suitable for low speeds, employed a lubrication supply system. Prior to the testing procedure, the surfaces of both the block and the disk were cleaned through ultrasonic cleaning in ethanol and dried in air. The standard deviation from the curves was utilized to calculate the error bars for the friction coefficient versus sliding distance.

The minimum film thicknesses were determined for the isothermal elastohydrodynamic lubrication conditions using the Hamrock and Dowson equation [89,90] given below (Equation (1)), which applies to linear contacts and various material combinations up to maximum pressures of 3 to 4 GPa [91].

$$\frac{h_0}{R'} = 3.63 \left(\frac{U\eta_0}{E'R'}\right)^{0.68} (\alpha E')^{0.49} \left(\frac{W}{E'R'^2}\right)^{-0.073} (1 - e^{-0.68k}) \quad (1)$$

where α is the pressure-viscosity coefficient, R' is the reduced radius of curvature, η_0 is the lubricant viscosity at atmospheric pressure and temperature, W is the applied load, E' is the reduced Young's modulus, U is the sliding speed, and k is the ellipticity parameter which is given by the ratio of semiaxis in the transverse direction to the semiaxis in the direction of motion, k is infinite for a line contact as in the case of a block-on-ring configuration. These were the parameters taken into consideration in the calculation of the film thickness. The lubricant fluid was assumed to be compressible, and its viscosity-pressure behavior was

described by the Barus law given below (Equation (2)) in which the lubricant viscosity η_p at pressure p and temperature θ was considered in the calculations.

$$\eta_p = \eta_0 e^{\alpha p} \tag{2}$$

To consider the effect of the surface roughness of both materials on the calculation of the film thickness, Tallian introduced a new parameter given below (Equation (3)) [92], which characterizes the ratio between the minimum film thickness and the combined surface roughness, represented by the symbol λ. The parameter λ is calculated as the ratio of the minimum film thickness to the composite surface roughness, where the surface roughness (Root Mean Square) of body A and body B is represented by σ_A and σ_B, respectively.

$$\lambda = \frac{h_0}{\sqrt{({\sigma_A}^2 + {\sigma_B}^2)}} \tag{3}$$

The criterion for lubrication regime determination values is summarized below [93,94]. The analysis of the λ value reveals distinct regimes and their corresponding lubrication conditions:

- λ > 5: Complete hydrodynamic lubrication
  - This regime indicates a lubrication condition where the lubricant film thickness is sufficient to entirely separate the surfaces, resulting in minimal wear and friction.
- 3 < λ < 5: Asperity smoothing, minimum wear
  - In this regime, the lubricant film thickness is moderate, allowing some contact between the surfaces. However, the pressure is high enough to deform the asperities, reducing wear and promoting smoother operation.
- 1.5 < λ < 3: Asperity smoothing
  - This regime represents a lubrication condition with a relatively thin lubricant film, allowing some contact between the surfaces. However, the pressure is insufficient to prevent direct contact between the asperities.
- 1 < λ < 1.5: Asperity smoothing, delamination
  - Similar to the previous regime, this regime involves asperity smoothing but with an additional factor of delamination. Delamination refers to the separation of thin surface layers under specific conditions.
- λ < 1: Macro-Plastic deformation
  - The regime indicates a lubrication condition where the lubricant film thickness is extremely thin or absent, leading to direct contact between the surfaces. This regime is characterized by significant plastic deformation of the contacting asperities.

As previously discussed, increasing the lubricant viscosity leads to a transition from boundary to mixed and hydrodynamic lubrication regimes at lower speeds.

The acquisition of hardness and reduced Young's modulus was achieved through the process of nano-indentation, utilizing a Berkovich diamond indenter within the nano indenter device. To guarantee that the indentation depth would not exceed 10% of the coating thickness, a maximum load of 10 mN, in accordance with the standard parameters of the CEMMPRE laboratory, was applied. The mechanical properties were determined by calculating the mean and standard deviation based on sixteen measurements that were conducted on each sample.

The various conditions of block on ring tribological test at different sliding speeds and sliding times can be found in Table 1. These conditions are specifically selected to plot the points for Stribeck curve.

Table 1. Conditions for block on ring tribological test.

		1	2	3	4	5
Conditions	Potentiometer	1.6	4.9	11.2	24.7	45.5
	Sliding Speed (m/s)	0.02	0.07	0.18	0.40	0.74
	Rotational speed (rpm)	4	13	32	64	127
	Rotational speed (rps)	0.07	0.21	0.53	1.06	2.12
	Number of turns	100	250	500	1000	1000
	Sliding time (s)	1500	1181	943	942	471

3. Results and Discussion

3.1. Viscosity of Lubricants

To investigate the temperature responses of various ILs, a viscosity test was conducted from 100 °C to ambient temperature of 25 °C on both the lubricants with ionic liquids as additives. Different ionic liquids have distinct temperature responses due to variations in their structural features, including the size, symmetry, and presence of specific functional groups. Understanding these temperature-dependent behaviours is essential, therefore, In the study of lubricated contacts, the viscosity is considered a crucial factor as it influences the tribological characteristics of the lubricants [95].

Figures 5 and 6 below show the viscosity/temperature relation of both the lubricants with ionic liquids as additives. In this investigation, variations in viscosity were observed due to the utilization of differing temperatures in the tests as well as due to the different composition of ionic liquid additives.

Comparatively, the viscosity of PAO 8 is 8% to 20% lower than its counterpart with the addition of ionic liquids {[P_{66614}][DEHP]} and {[EMIM][DEP]}. Even though just being at 1% the weight of the lubricant, it has some significant change in the viscosity and the action of lubricant of the surface. Of all the lubricants, {[P_{66614}][DEHP]} has highest viscosity, followed by {[EMIM][DEP]}. This is due to the different viscosities of the ionic liquids themselves. The viscosity of the ionic liquid is influenced by its structural characteristics. The viscosity is enhanced as the side chain lengthens or as the cation's symmetry increases. Additionally, an increase in the number of branches leads to a corresponding increase in the viscosity [96].

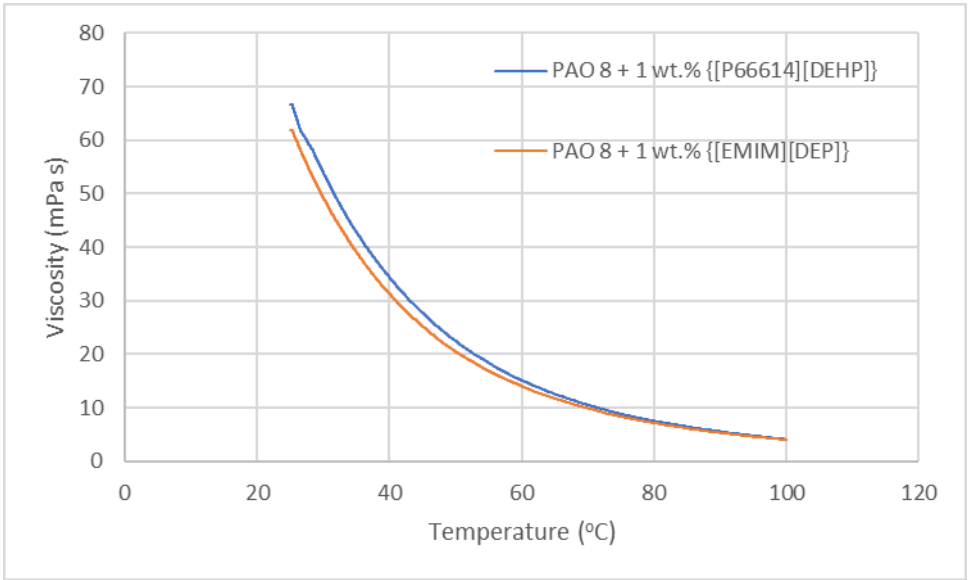

Figure 5. Viscosity/temperature graph of PAO 8 + 1 wt.% {[P_{66614}][DEHP]} and PAO 8 + 1 wt.% {[EMIM][DEP]}.

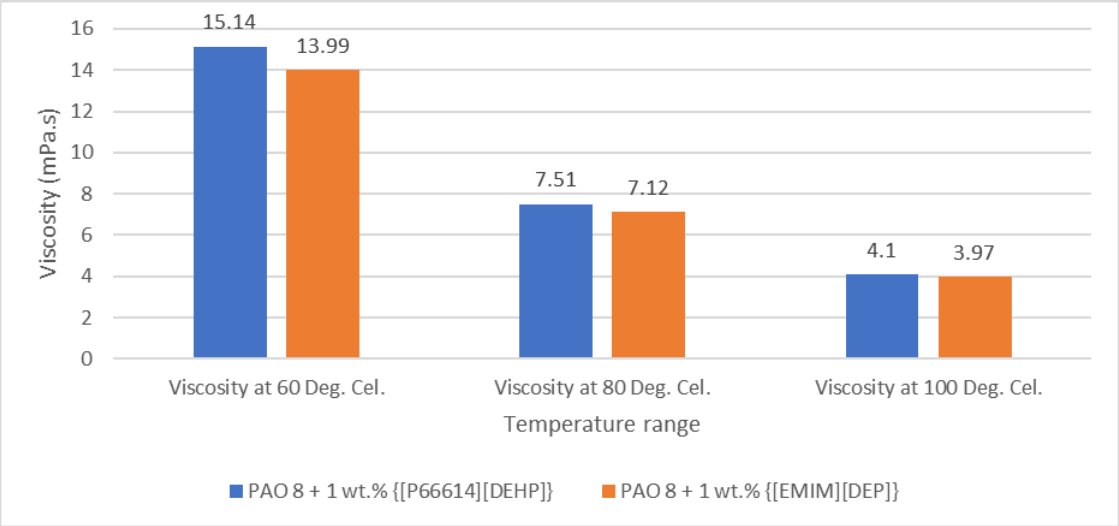

Figure 6. Viscosity/temperature relation of lubricants.

Ionic liquid {[P_{66614}][DEHP]} has 7.6% higher viscosity at 60 Degree Celsius compared to {[EMIM][DEP]} but the difference reduces to being negligible as the temperature increases. A slightly higher viscosity from the ionic liquids {[P_{66614}][DEHP]} and {[EMIM][DEP]} has benefited by extending some portion of the Stribeck curve in the mixed lubrication regime which will be discussed in the further section of Stribeck curves. The analysis revealed that different ionic liquids exhibit diverse temperature responses, primarily due to the structural variations of their constituent ions [97]. ILs with smaller, more symmetrical cations and anions tend to have higher melting points and exhibit less temperature dependence. In contrast, ILs composed of bulkier, asymmetric ions generally display lower melting points and a greater sensitivity to temperature variations [97].

Furthermore, the presence of specific functional groups in the IL structure can influence the temperature response [98]. For example, ILs containing hydrogen bond acceptors and donors exhibit increased ionic conductivity and can display significant changes in properties with temperature variations, including viscosity and solubility [98]. Additionally, the type and strength of intermolecular interactions within the IL, such as ion-ion interactions, ion-dipole interactions, and hydrogen bonding, contribute to the temperature-dependent behavior [99]. These interactions affect the ordering and dynamics of the ions, influencing the overall response to temperature changes.

3.2. Mechanical Characterization (Hardness and Young's Modulus)

Figures 7 and 8 show, respectively, the hardness and Young's modulus for the three different DLC coatings. As seen in Figure 5, the highest result of hardness was obtained for Pure DLC, exhibiting a mean value of approximately 21 GPa, while the mean value for Eu-DLC with an atomic concentration of 2.4% was found to be around 19.37 GPa and that of 2.3% Gd-DLC is 19.62 GPa. The reduced Young's modulus of the DLC coatings was observed to be between 180 and 195 GPa and can be seen in Figure 6. These values of hardness and Young's modulus were determined to be comparable to those of pure DLC coatings produced using the same technique by Ji Cheng et al. [100]. Consequently, it was concluded that despite the addition of dopant elements, the mechanical properties of the coatings were not affected.

The variations in hardness and Young's modulus can be attributed to morphological type, sp^2 or sp^3 hybridization, and structural evaluation through density analysis. The high hardness in DLC coatings can be achieved with a high proportion of sp^3 hybridization in the amorphous carbon matrix and a dense and compact structure in the DLC coating [101–104]. Nevertheless, a decrease in the sp^3/sp^2 ratio results in a reduction in the hardness of DLC coatings [105].

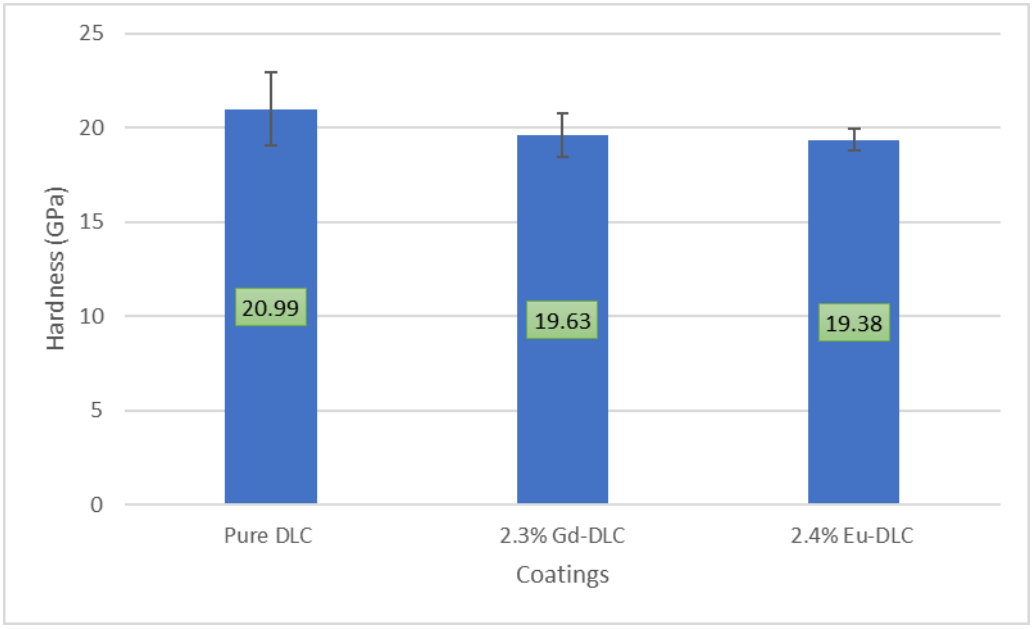

Figure 7. Hardness of coatings.

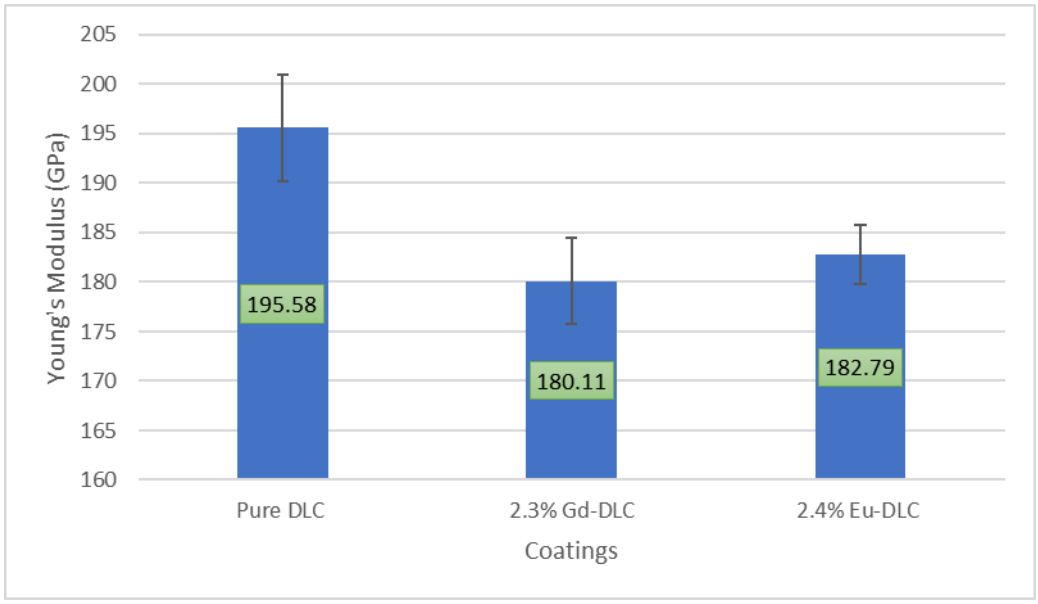

Figure 8. Young's Modulus of coatings.

3.3. Tribological Test (Influence of the Temperature)

The results of the block on ring tribotests are divided into three groups based on the temperature (60 °C, 80 °C and 100 °C). In these three temperature groups we can find the specific coating along with which lubricant was tested. The calculation of the Hersey parameter was performed by multiplying the viscosity of the lubricating oil at various temperatures by the sliding speed applied during the tests and dividing the result by the normal force (25 N) per unit length (12 mm). The Stribeck curves were generated from the values of the coefficient of friction obtained from tests conducted at different sliding speeds and temperatures with different DLC coatings. The standard deviation values, as we will see, were found to be minimal for all points and showed a tendency to decrease with increasing sliding speed, thus only the average data set was presented. Analysis of these curves revealed the existence of three lubrication regimes: boundary, mixed, and hydrodynamic lubrication.

3.3.1. Temperature of 60 °C

Table 2 presents the Tallian parameter along with the film thickness calculated from the Hamrock and Dowson equation for 60 °C. It is possible to observe that the PAO8 + 1 wt.% {[P_{66614}][DEHP]} presents the highest film thickness and lambda parameter. This is followed by PAO8 + 1 wt.% {[EMIM][DEP]}.

Table 2. Tallian parameter and film thickness at 60 °C.

T = 60 °C						
	Sliding speed—u (m/s)	0.0241	0.0765	0.1916	0.3835	0.7671
PAO 8 + 1 wt.% {[P_{66614}][DEHP]}	Film Thickness—h_0 (m)	1.97×10^{-8}	4.32×10^{-8}	8.06×10^{-8}	1.29×10^{-7}	2.07×10^{-7}
	Tallian Parameter—λ	0.3226	0.7077	1.3213	2.1184	3.3939
PAO 8 + 1 wt.% {[EMIM][DEP]}	Film Thickness—h_0 (m)	1.87×10^{-8}	4.1×10^{-8}	7.65×10^{-8}	1.23×10^{-7}	1.96×10^{-7}
	Tallian Parameter—λ	0.3058	0.6710	1.2528	2.0086	3.2180

Figure 9 presents the evolution of the coefficient of friction with Hersey number (Stribeck curve) for the different DLC coatings under different lubricating conditions at 60 °C.

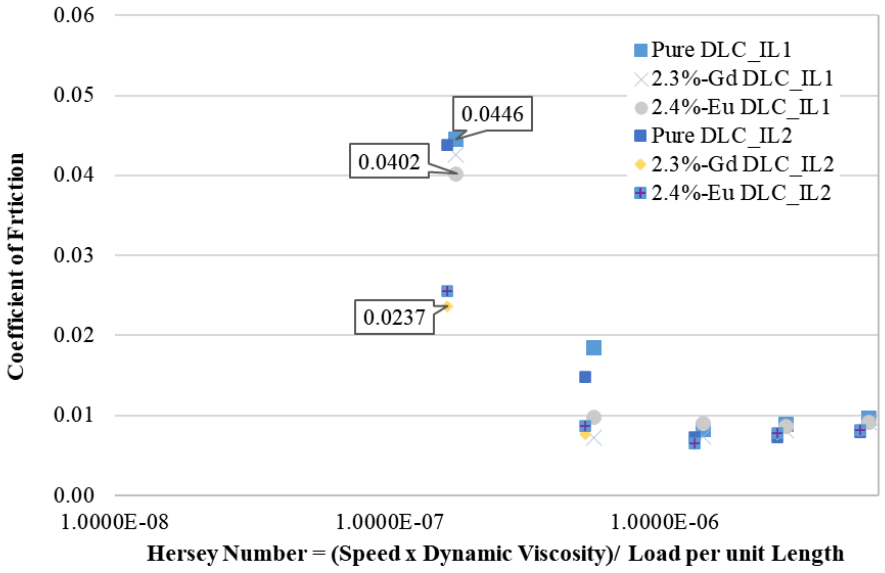

Figure 9. Stribeck Curve at 60 °C.

There is 46.86% of reduction in the coefficient of friction using ([EMIM][DEP]) as ionic liquid additive in PAO8 and the doped DLC with Gadolinium at a very low speed of (0.02 m/s) in boundary lubrication condition compared to the Pure DLC with PAO 8 + 1 wt.% {[P_{66614}][DEHP]}. Specifically, ([EMIM][DEP]) has shown a significant consistency in lowering the friction levels. Pure DLC and ionic liquid additives show a contrasting behavior with high CoF (0.0446) which is 47% higher compared to the doped DLCs in similar condition of 60 °C. This proves that the ionic liquid along with the doped elements have some interaction between them which creates a tribofilm and is preventing the asperity-asperity contact on the surface.

In elastohydrodynamic region, all the points converge which suggest a uniform lubrication film thickness. The distinctive points are the first two, which are in boundary lubrication condition. The thickness of the lubrication film in the elastohydrodynamic regime ($3 < \lambda < 5$) is thinner than the hydrodynamic regime ($5 < \lambda$), and in the results we

do not find any point of λ parameter greater than 5, therefore it is in elastohydrodynamic regime. Consequently, the maintenance of an uninterrupted hydrodynamic film necessitates the elastic deflection of the surfaces. Therefore, when studying elastohydrodynamic region, it becomes imperative to consider these deflections [106,107]. In the hydrodynamic lubrication regime, characterized by a lambda ratio greater than 5, the load is entirely supported by the lubricant film, and there is no contact between the asperities on the sliding surfaces [108,109].

In both the elastohydrodynamic and hydrodynamic regimes, as the speed escalates, the lubricating film may fail to match the pressure variations promptly, impeding the lubricant from adequately flowing into the contact area and forming a sufficiently thick fluid film. Consequently, this situation leads to an increase in friction [62,110]. Additionally, the viscosity of the lubricant commonly decreases as the temperature rises, which can occur occasionally during high sliding speeds due to the generation of heat resulting from friction, this will be represented further below for 80 and 100 °C.

3.3.2. Temperature of 80 °C

In Table 3 at 80 °C, there is no more elastohydrodynamic lubrication regime in both the lubricants. PAO 8 + 1 wt.% {[P_{66614}][DEHP]} outperforms other with highest film thickness (1.29×10^{-7} m) and Tallian parameter (2.1070) which is followed by PAO8 + 1 wt.% {[EMIM][DEP]} at (2.0319). In this case of 80 degree Celsius there will be mostly delamination and asperity smoothing. As the velocity will further decrease it will result in macro plastic deformation.

Table 3. Tallian parameter and film thickness at 80 °C.

T = 80 °C						
	Sliding speed—u (m/s)	0.0241	0.0765	0.1916	0.3835	0.7671
PAO 8 + 1 wt.% {[P_{66614}][DEHP]}	Film Thickness—h_0 (m)	1.22×10^{-8}	2.68×10^{-8}	5.01×10^{-8}	8.03×10^{-8}	1.29×10^{-7}
	Tallian Parameter—λ	0.2002	0.4393	0.8202	1.3151	2.1070
PAO 8 + 1 wt.% {[EMIM][DEP]}	Film Thickness—h_0 (m)	1.18×10^{-8}	2.59×10^{-8}	4.83×10^{-8}	7.74×10^{-8}	1.24×10^{-7}
	Tallian Parameter—λ	0.1931	0.4237	0.7910	1.2683	2.0319

From Figure 10 it is possible to observe that the curves are shifted towards the left side. As the temperature is increasing the Stribeck curve is shifting towards the mixed lubrication regime. The significant role played by the mixed lubrication regime ($1 < \lambda < 3$) in numerous close clearance machines cannot be understated. It encompasses a fusion of characteristics from both elastohydrodynamic lubrication and boundary lubrication. This signifies that while certain sections of the contact area are coated with a film of lubricant, other regions witness the sliding of peak asperities on the moving surfaces due to the absence of a separating liquid film. Engine components like piston rings, cams, and engine bearings frequently experience mixed lubrication. For system engineers, a comprehensive understanding of mixed lubrication is of utmost importance, as it represents the most demanding lubrication regime to accurately predict friction. This complexity arises from the intricate interplay between surface topography and the thickness of the oil film [106,111,112].

Gadolinium doped DLC with PAO 8 + 1 wt.% {[EMIM][DEP]} at 80 °C has shown a 30% substantial reduction in CoF in comparison to Pure DLC. The tribosytem composed of 2.4% Europium doped DLC also showed a similar result. Gadolinium (2.4%) doped DLC with PAO 8 + 1 wt.% {[P_{66614}][DEHP]} perform better than the Europium doped DLC. PAO 8 + 1 wt.% {[EMIM][DEP]} shows consistent results with all 5 DLC coatings with 2.3% Gd DLC and 2.4% Eu DLC being the best performing coatings.

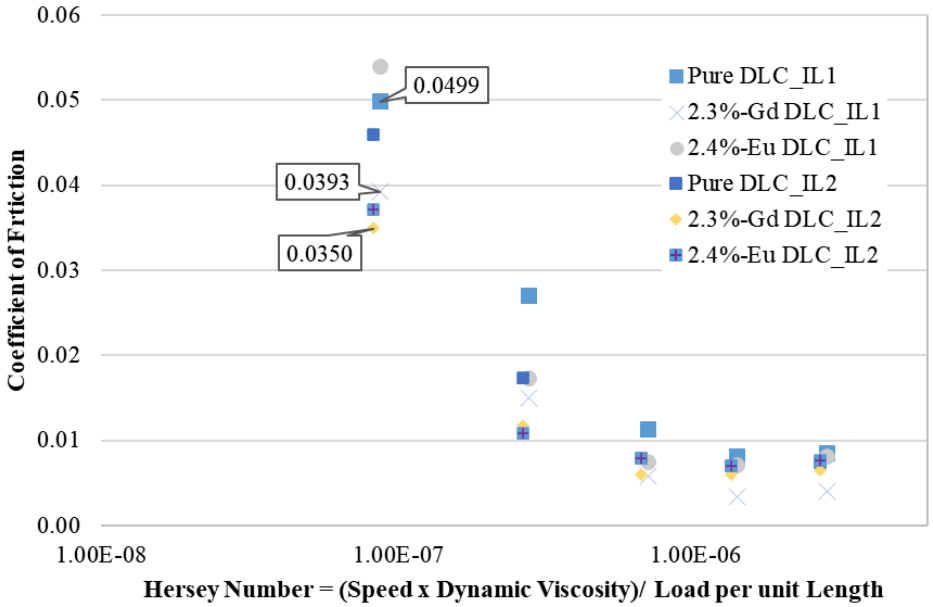

Figure 10. Stribeck Curves at 80 °C.

3.3.3. Temperature of 100 °C

It is an extreme condition with all the points in boundary lubrication regime with just last point on the brink of mixed lubrication which can be seen from the calculated Tallian parameters in Table 4. Certainly, in this case there will be asperity-asperity contact with macro plastic deformation on the surface.

Table 4. Tallian parameter and film thickness at 100 °C.

T = 100 °C						
	Sliding speed—u (m/s)	0.0241	0.0765	0.1916	0.3835	0.7671
PAO 8 + 1 wt.% {[P_{66614}][DEHP]}	Film Thickness—h_0 (m)	8.1×10^{-9}	1.78×10^{-8}	3.32×10^{-8}	5.32×10^{-8}	8.52×10^{-8}
	Tallian Parameter—λ	0.1327	0.2911	0.5435	0.8714	1.3961
PAO 8 + 1 wt.% {[EMIM][DEP]}	Film Thickness—h_0 (m)	7.92×10^{-9}	1.74×10^{-8}	3.25×10^{-8}	5.2×10^{-8}	8.34×10^{-8}
	Tallian Parameter—λ	0.1298	0.2848	0.5317	0.8525	1.3658

100 °C is an extreme condition and machines usually do not work at 100 Degree Celsius as there is constant cooling provided. As we can see the Stribeck curve in Figure 11, it is now completely into the boundary regime, except the last point which is marginally in mixed lubrication regime according to the Tallian parameter.

The boundary lubrication regime, with a coefficient λ less than 1, exhibits the feature of load support by the minute surface irregularities, without the presence of a continuous film of lubricant. The interaction between these irregularities can lead to substantial levels of friction and wear, ultimately diminishing the operational life of the system [106,109,113,114] and at 100 °C it is clearly evident. A 2.3% Gd DLC with PAO 8 + 1 wt.% {[P_{66614}][DEHP]} and PAO 8 + 1 wt.% {[EMIM][DEP]} at 100 °C has boundary friction of just 0.0379, compared that to with Pure DLC which is 0.0505, a total of 25% improved performance in coefficient of friction with ionic liquids and doping.

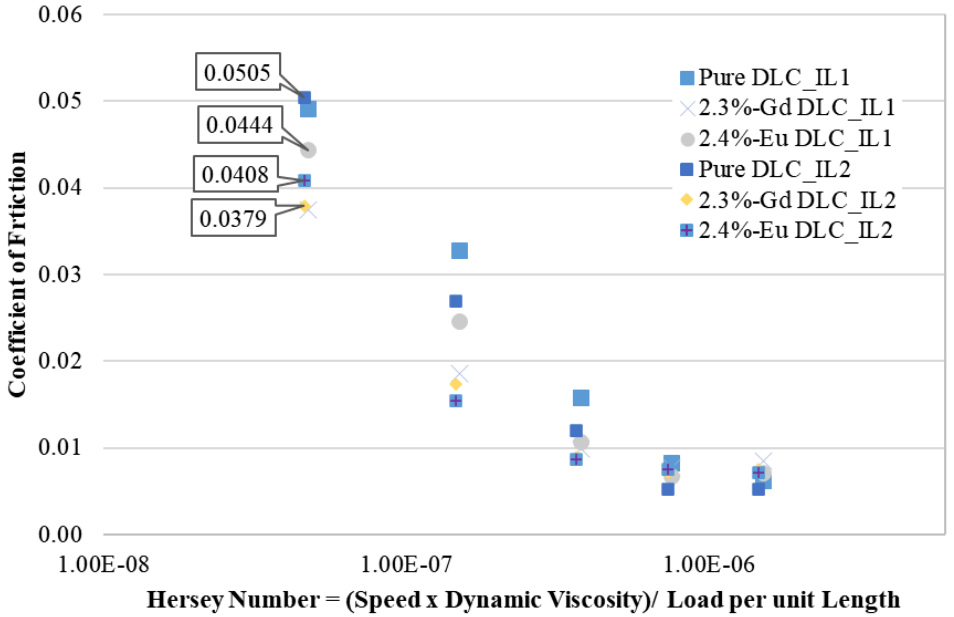

Figure 11. Stribeck Curves at 100 °C.

2.4% Eu DLC performs better with PAO 8 + 1 wt.% {[EMIM][DEP]} at 100 Deg. Celsius whereas, pure DLC has the worst performing trend in all the three lubricants. Even at very high temperatures of 100 degrees Celsius the coefficient of friction has no drastic increase which suggests that the DLC coatings are interacting with lubricants to keep the friction as low as possible. Out of all 2.3% Gd DLC along with PAO 8 + 1 wt.% {[P_{66614}][DEHP]} has proven to be the best combination with the least coefficient of friction.

When comparing the Stribeck curves of different films, it was found that adding the ionic liquid to the PAO 8 lubricant generally decreased the coefficient of friction (CoF) at the lowest achievable sliding speed. This effect was particularly significant for the Gd-doped DLC film. The Eu-DLC film exhibited improved performance compared to the pure DLC film when the ionic liquid was present. The primary factor responsible for the reduced CoF in Eu-DLC and Gd-DLC films is the formation of adsorbed layers. These layers facilitate movement between two sliding surfaces due to their low shear. Additionally, the formation of a protective tribofilm on metal surfaces, resulting from chemical reactions between ionic liquids and the contacting surfaces during friction, is another contributing factor discussed [43,115]. As per the proposed mechanism for adsorbed layers, the negatively charged part of ionic liquids is attracted to the positively charged metal surface, causing adsorption on the surface [116]. Another anionic entity can adsorb the cationic component, resulting in the formation of single- or multi-layered adsorbed structures on the surface. These structures generate a film on the metal surface and possess weak bonding between the layers, which aids in decreasing friction and facilitates movement between the surfaces in contact [43,115,117,118].

3.4. Wear Mechanism Characterization

SEM-EDS was used to assess the impact of incorporating an ionic liquid (IL) as an additive on the characteristics of diamond-like carbon (DLC) thin films. SEM-EDS images of Gd-DLC and Eu-DLC films are depicted in Figures 12–18. These maps reveal that the thin film was partially removed in certain regions, and the presence of chromium, originating from the interlayer, was detected. At the location of wear, we can clearly see the distinction of the elements from each other.

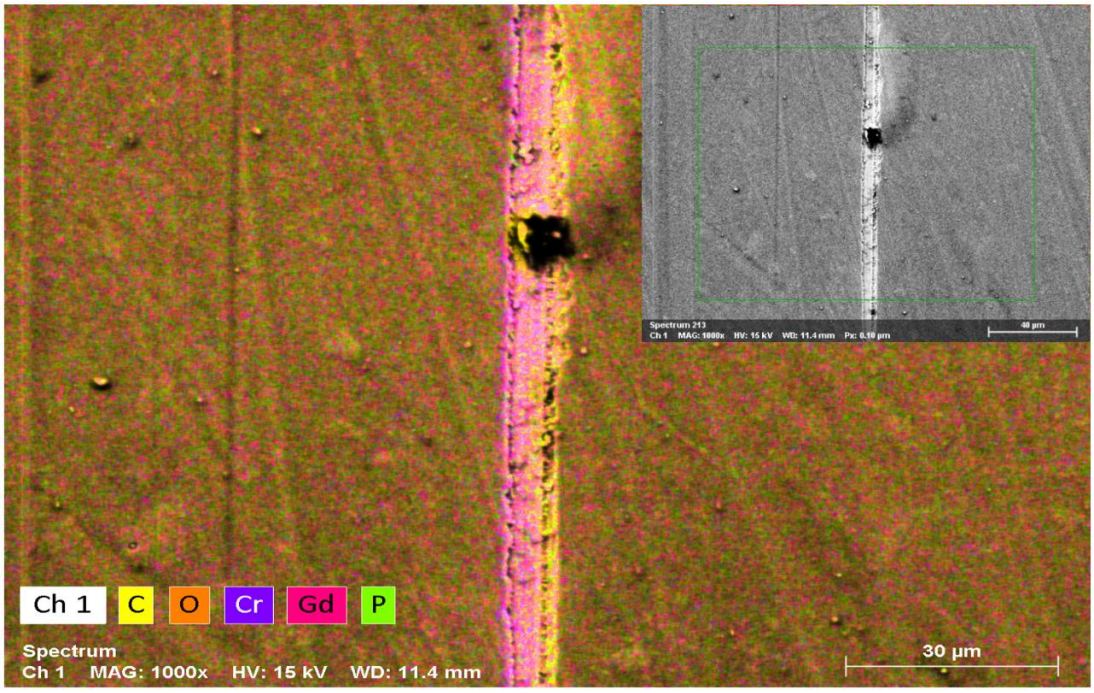

Figure 12. EDS of 2.3% Gd-DLC with IL#1 and SEM image of the same in top right corner.

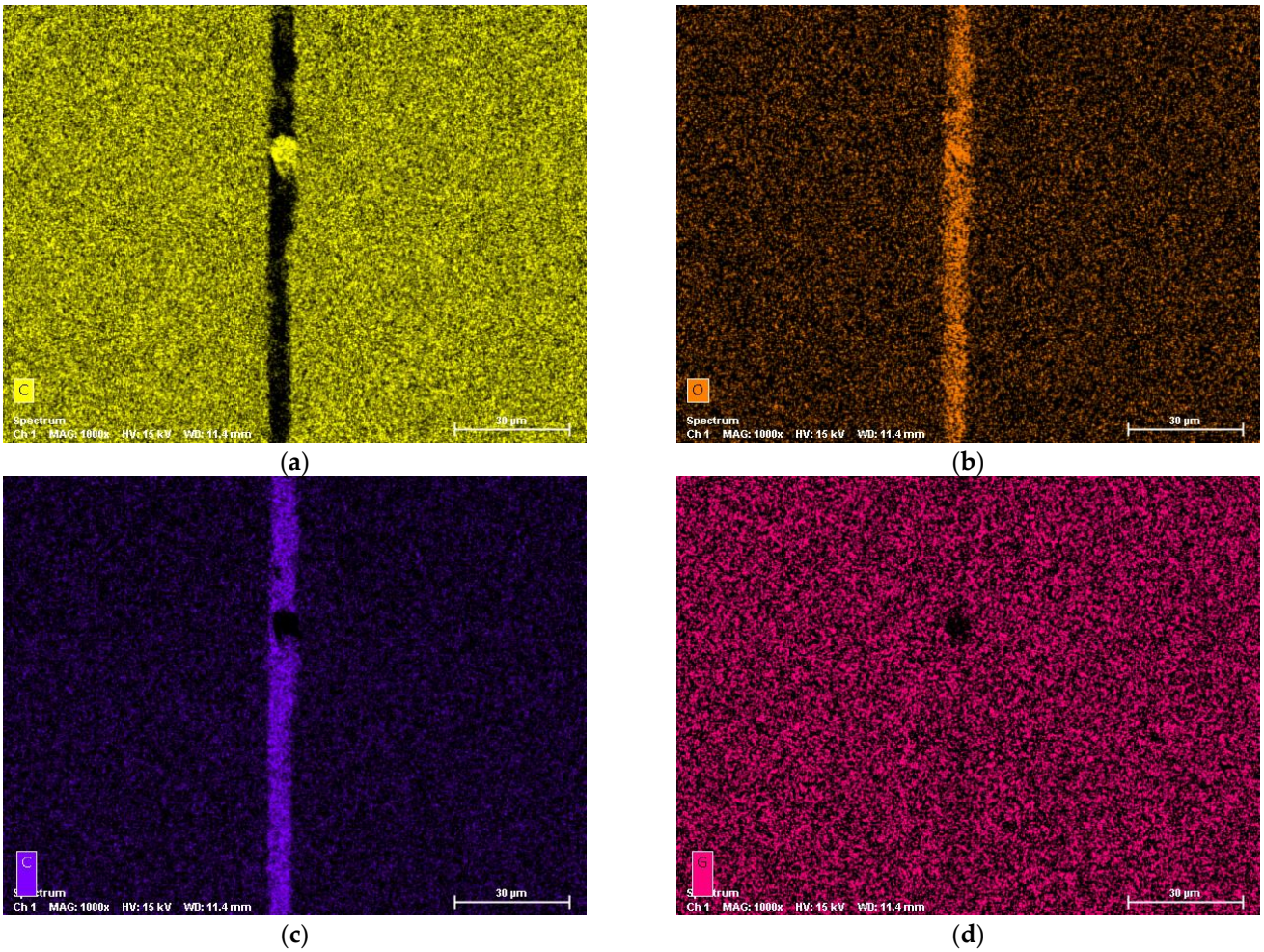

(**a**) (**b**)

(**c**) (**d**)

Figure 13. *Cont.*

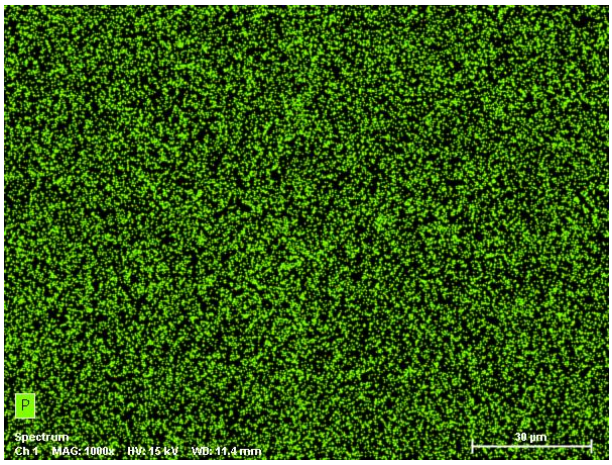

(**e**)

Figure 13. Element mapping of the Gd-DLC thin film paired with PAO 8 + 1 wt. % IL#1: (**a**) C; (**b**) O; (**c**) Cr; (**d**) Gd and (**e**) P.

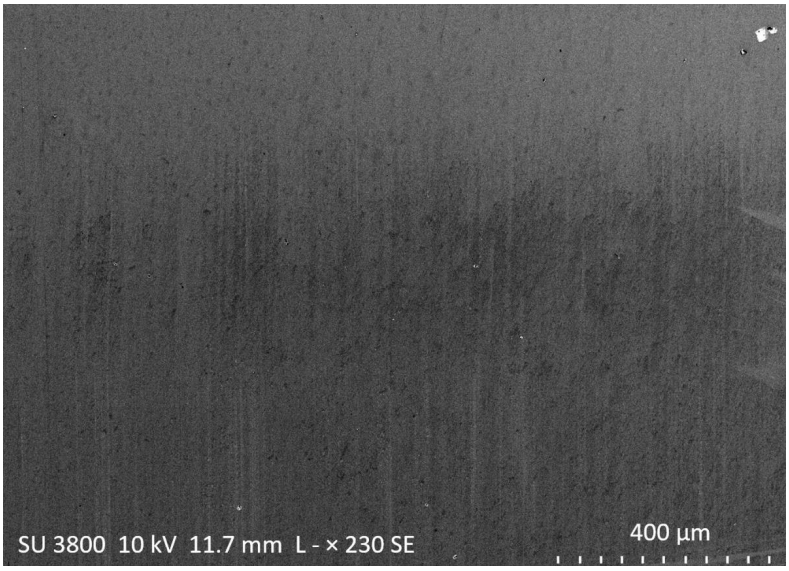

Figure 14. Scratch/Wear pattern on 2.4% Eu DLC coating with PAO 8 + 1 wt.% {[EMIM][DEP]}.

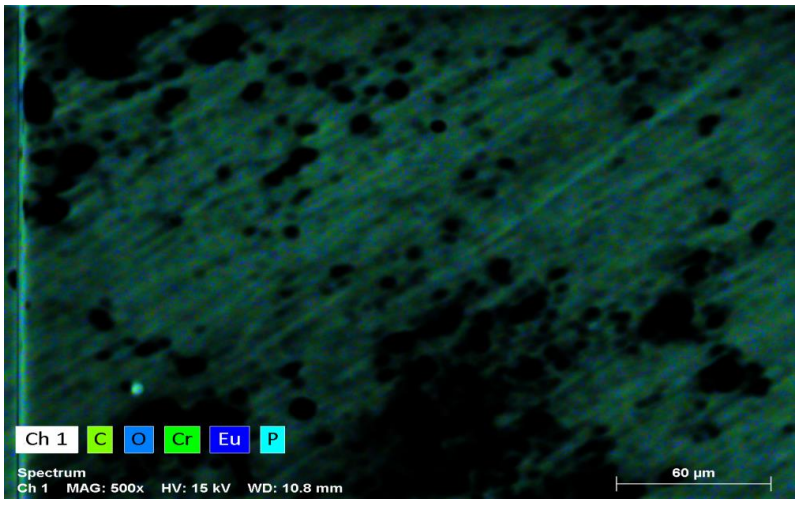

Figure 15. EDS image of oxides on the 2.4% Eu-DLC surface PAO 8 + 1 wt.% {[P_{66614}][DEHP]}.

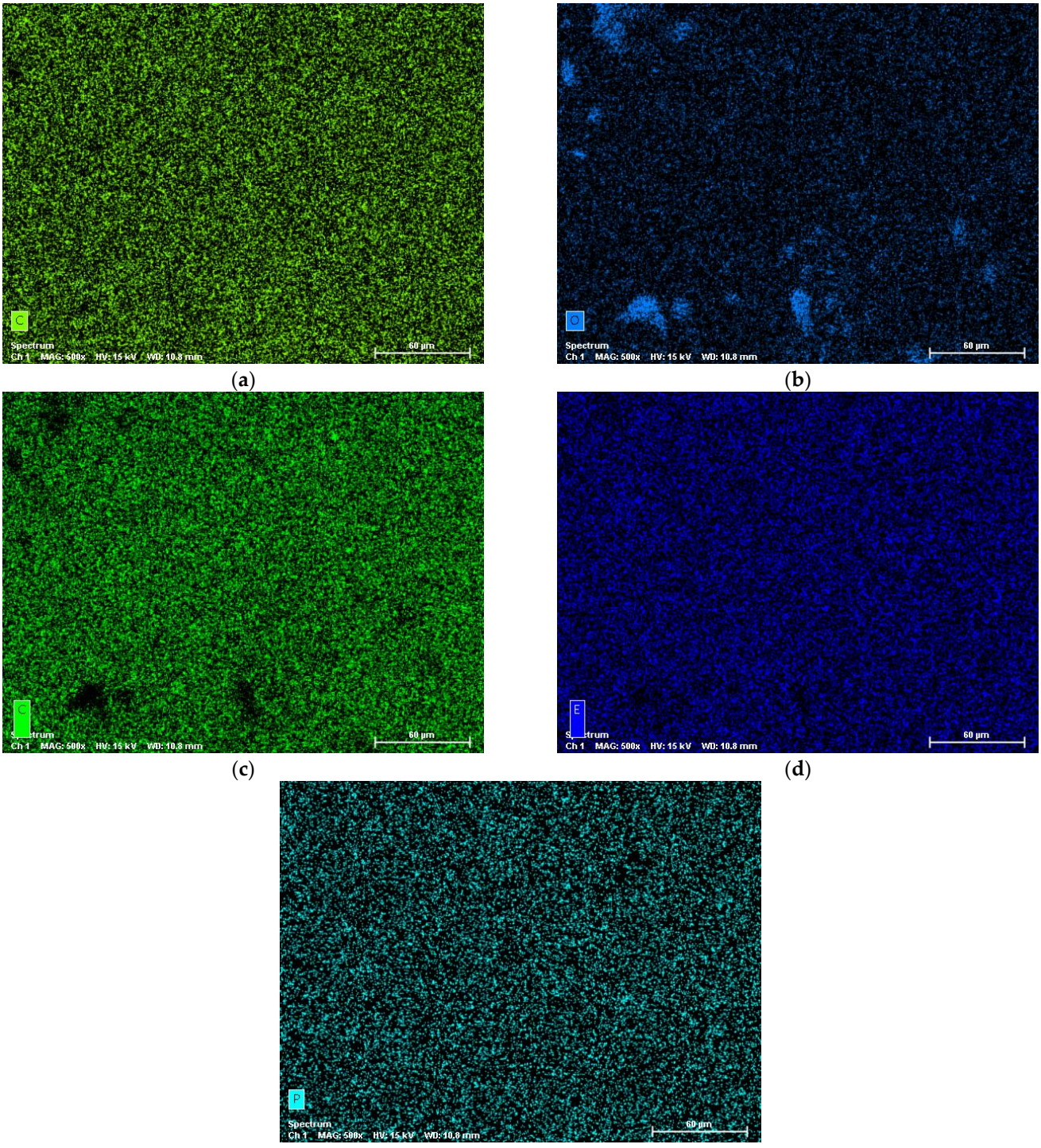

Figure 16. EDS X Ray map of oxides on the 2.4% Eu-DLC surface PAO 8 + 1 wt.% {[P_{66614}][DEHP]} surface: (**a**) C; (**b**) O; (**c**) Cr; (**d**) Eu; and (**e**) P.

Figures 12 and 13 show the EDS X Ray mapping which gives us the details of the elements for 2.3% Gd DLC sample with PAO8 + 1 wt.% {[P_{66614}][DEHP]}. The sample was kept constant for the lubricant and was rotated at 45-degree angle for the three temperature ranges, this method was adopted to maintain the steady state conditions. The SEM-EDS analysis was performed at the end of performing all the experiments, but it is difficult to contemplate the temperature regions. Therefore, the sample results represent an overall view of the entire temperature range.

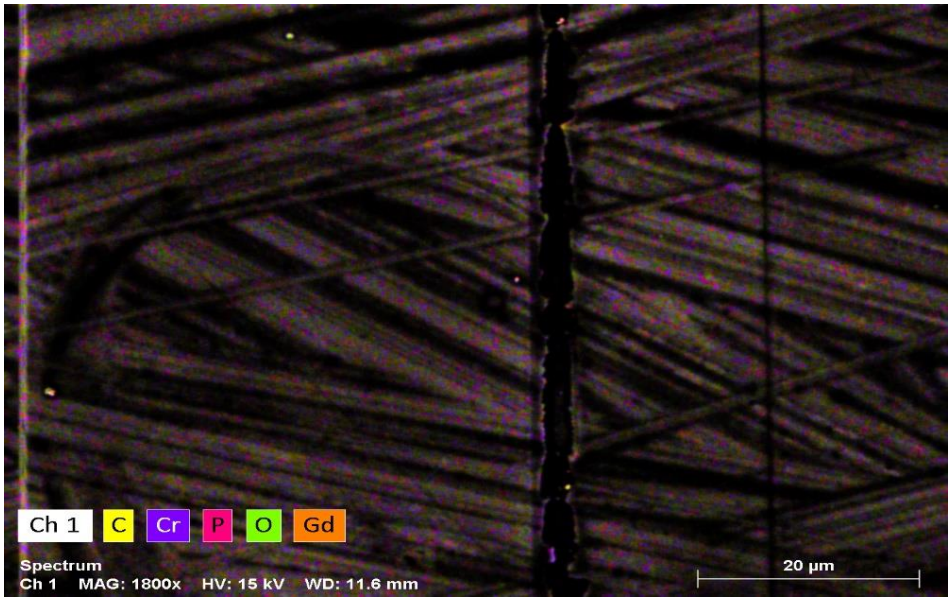

Figure 17. EDS image of oxides on the 2.3% Gd-DLC with PAO 8 + 1 wt.% {[EMIM][DEP]}.

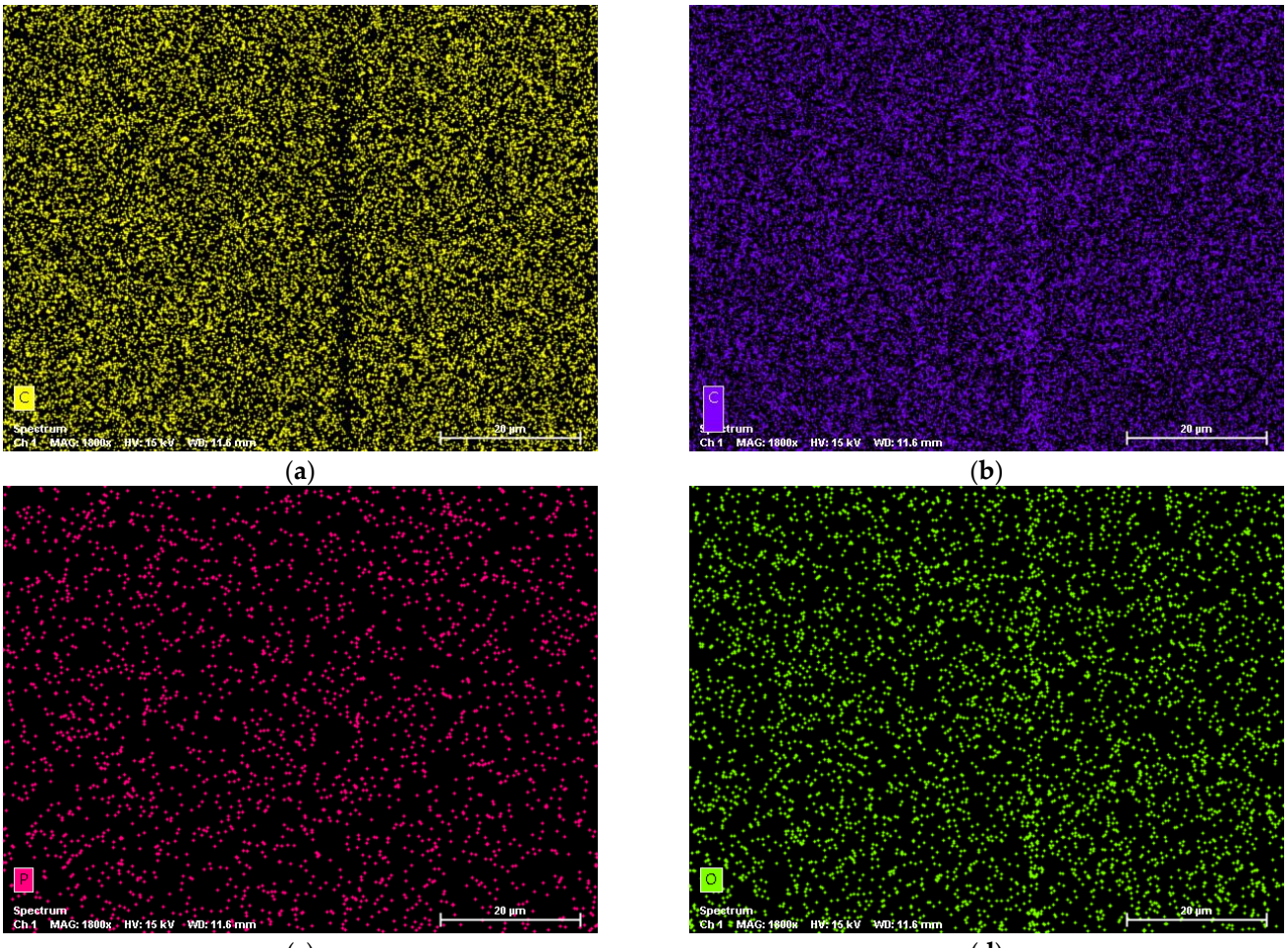

Figure 18. *Cont.*

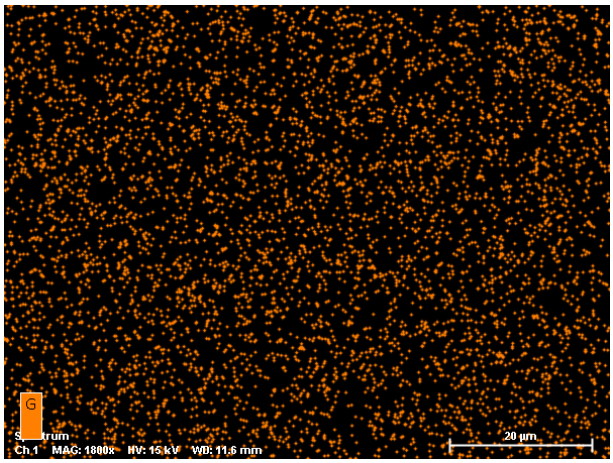

(**e**)

Figure 18. EDS X Ray map of oxides on the 2.3% Gd-DLC with PAO 8 + 1 wt.% {[EMIM][DEP]} surface: (**a**) C; (**b**) Cr; (**c**) P; (**d**) O; and (**e**) Gd.

In the results we can see, Chromium (purple) is the interlayer of CrN and Carbon (yellow) is from the DLC coating, Gadolinium (pink) is the dopant, Phosphorous (green) is from the ionic liquid. Calculation of the wear rate is not possible as the wear is not uniform and is difficult to identify a wear track. However, from a general overview in the SEM, Gd-DLC has some significantly visible wear, whereas Eu-DLC has less to no wear on the samples. A study performed by M Sadeghi. et.al. shows the similar results found in the optical microscopy images of different lubricant films along with SEM-EDS images, the wear reduction is clearly evident by using ionic liquids as additives and doping of DLC coatings [74].

The 2.4% Eu DLC with PAO8 + 1 wt.% {[EMIM][DEP]} have significantly performed better with the least CoF even at the extreme conditions of 100 Degree Celsius, it can also be seen in the SEM image that the coating has no wear but a light bruise/scratch.

The SEM-EDS technique was used to assess the impact of IL with 2.3% Gd-DLC and 2.4% Eu-DLC. On 2.4% Eu-DLC with PAO 8 + 1 wt.% {[P_{66614}][DEHP]} sample, oxides were found on the surface and there were no significant wear marks. This suggested the formation of tribofilm through oxides, although there is no direct evidence of tribofilm. In a study by Barnhill et al. [20], it was discovered that the lubricants containing [P_{66614}][DEHP] had a tribofilm containing oxygen and phosphorus. This finding suggests that the tribofilm originated from the [P_{66614}][DEHP]. In EDS X ray map in Figures 15 and 16, we can distinctly see the oxygen and a very slight presence of phosphorous, from which we can conclude that phosphorous based ionic liquid reacted with the surface of the Europium doped DLC coating to a form a tribofilm.

Gd-DLC also forms a tribofilm which can be inferred from EDS X ray map in Figures 17 and 18, oxides were found on the surface near the wear marks. This suggests the formation of tribofilm through oxides. In EDS X ray map we can distinctly see the oxygen and presence of phosphorous, from which we can conclude that phosphorous based ionic liquid reacted with the surface of the Gadolinium doped DLC coating to a form a tribofilm.

Research was conducted by Qu J. et.al on [P_{66614}][DEHP] and its interaction with a steel surface. The study, performed using TEM by Qu J. et.al, displayed a cross-section of the region just below the wear mark, which was lubricated by PAO + IL. The cross-section revealed a two-layer structure consisting of a top film at the boundary (120–180 nm) and a deeper zone (0.5–0.8 µm) exhibiting plastic deformation and a refined grain structure. The IL additive is believed to provide anti-scuffing and anti-wear properties through this protective boundary film. When the boundary film was observed at a higher magnification, it exhibited an amorphous matrix containing small nanoparticles (1–10 nm in diameter). The electron diffraction pattern confirmed the presence of a nanocomposite phase structure.

EDS element mapping indicated significant concentrations of P, O, and Fe in the boundary film, resulting from the interactions between the IL and the metal surface [44]. Similarly, our EDS elemental mapping shows P, O, and Eu/Gd resulting from the interactions between the IL and the coatings.

4. Conclusions

In summary, this study investigated the tribological performance of rare earth element-doped diamond-like carbon (DLC) coatings in the presence of ionic liquid additives under different temperature conditions. DLC coatings have been considered as a sustainable solution for reducing frictional losses in mechanical systems due to their excellent tribological and mechanical properties. However, pure DLC coatings are inert and do not interact effectively with conventional lubricants, resulting in wear and tear. To address this limitation, doping DLC coatings with metals has shown promise in enhancing their reactivity with lubricants. Ionic liquids have emerged as a potential solution due to their adjustable properties for specific applications and their ability to form protective tribofilms.

The study specifically examined the interaction between Europium and Gadolinium dopants in DLC coatings and ionic liquid additives in Polyalphaolefin 8 (PAO8). Two different lubricants were used in the experimental investigation to evaluate the tribological performance of the coatings under three different temperature conditions.

The results demonstrate that both ionic liquid additives can improve the tribological performance of DLC coatings. However, the optimal temperature range for each coating differs depending on the doping element and the type of ionic liquid used.

At 60 degrees Celsius, the combination of 2.3% Gadolinium-doped DLC with PAO 8 + 1 wt.% {[EMIM][DEP]} showed the best results with the lowest coefficient of friction (CoF), followed by 2.4% Europium-doped DLC. The addition of {[EMIM][DEP]} resulted in a more significant reduction in the coefficient of friction compared to {[P_{66614}][DEHP]}, although the latter showed a lower wear rate (wear rate from the general overview from the SEM-EDS analysis as the calculation of wear rate is not possible as explained earlier). The 2.3% Gadolinium-doped DLC and 2.4% Europium-doped DLC coatings consistently exhibited superior tribological performance under all conditions compared to the Pure DLC, highlighting the beneficial effects of rare earth metal doping.

Nevertheless, as we move in the higher temperature range, it has significant reduction in coefficient of friction, which is also in line with prior research on iron/steel substrates, [P_{66614}][DEHP] demonstrates commendable performance at elevated temperatures [44–46].

At 80 degrees Celsius, both dopants with PAO 8 + 1 wt.% {[EMIM][DEP]} showed a substantial decrease in the coefficient of friction compared to Pure DLC. The lubricant plays a crucial role in providing the necessary film between the contacting surfaces, and the ionic liquid additives enhance the overall performance of the coatings. The 2.4% Gadolinium-doped DLC with PAO 8 + 1 wt.% {[P_{66614}][DEHP]} outperformed the Europium-doped DLC under these conditions. Also, the results of Omiya et al. are in good harmony with this study, it also revealed that as the concentration of the dopant increases in the DLC coatings, there is significant improvement with reduction in CoF and wear rate [73].

In extreme conditions of 100 degrees Celsius, all the points were within the boundary lubrication regime, except the last point, which was marginally in the mixed lubrication regime. The DLC coatings, even at high temperatures, demonstrated low coefficients of friction, indicating their effective interaction with the lubricants. Among all the combinations, the 2.3% Gadolinium-doped DLC with PAO 8 + 1 wt.% {[P_{66614}][DEHP]} exhibited the best performance with the lowest coefficient of friction. The most feasible answer to these results is that ionic liquids maintain their viscosity index and properties quite well as compared to base oil, moreover from the research performed by Fontes et.al., it indicated the high performance derived by using the combination of Eu-DLC and Gd-DLC with the ionic liquids [72].

The SEM-EDS analysis confirms the performance of the Eu-DLC with a very light scratch whereas the Gd-DLC has some wear marks. The element in the EDS also shows the

formation of oxides, which strongly suggest that there is interaction between the coatings and the ionic liquids. The prior research of pure PAO 8 as reference and PAO 8 additivated with {[P_{66614}][DEHP]} by M. Sadeghi has shown the similar results with drastic reduction in wear and CoF [74].

Overall, the findings of this study highlight the potential of rare earth element-doped DLC coatings and ionic liquid additives for improving tribological performance in various temperature conditions. The results contribute to the understanding of the interactions between DLC coatings, dopants, and lubricants, providing valuable insights for the development of advanced lubrication systems with enhanced friction and wear properties.

Author Contributions: Conceptualization, A.C., A.R. and F.F.; Methodology, A.R. and F.F.; Formal analysis, T.O. and L.V.; Investigation, S.S. and L.V.; Resources, A.R. and F.F.; Writing—original draft, S.S.; Writing—review & editing, T.O., L.V. and F.F.; Supervision, F.F.; Project administration, F.F.; Funding acquisition, F.F. All authors have read and agreed to the published version of the manuscript.

Funding: Thisresearch was funded by FEDER funds through the program COMPETE—Programa Operacional Factores de Competitividade, by national funds through FCT–Fundação para a Ciência e a Tecnologia, under the project UIDB/00285/2020, LA/P/0112/2020, SmartHyLub (2022.05603.PTDC), and by the Taiho Kogyo Tribology Research Foundation (Grant No. 22A25).

Data Availability Statement: The data presented in this study are available on request from the corresponding author.

Conflicts of Interest: The authors declare no conflict of interest.

References

1. Holmberg, K.; Erdemir, A. The Impact of Tribology on Energy Use and CO_2 Emission Globally and in Combustion Engine and Electric Cars. *Tribol. Int.* **2019**, *135*, 389–396. [CrossRef]
2. Holmberg, K.; Andersson, P.; Erdemir, A. Global Energy Consumption Due to Friction in Passenger Cars. *Tribol. Int.* **2012**, *47*, 221–234. [CrossRef]
3. Zichao, L.; Bin, S.; Fanghong, S.; Zhiming, Z.; Songshou, G. Diamond-Coated Tube Drawing Die Optimization Using Finite Element Model Simulation and Response Surface Methodology. *Proc. Inst. Mech. Eng. B J. Eng. Manuf.* **2014**, *228*, 1432–1441. [CrossRef]
4. Santiago, J.A.; Fernández-Martínez, I.; Sánchez-López, J.C.; Rojas, T.C.; Wennberg, A.; Bellido-González, V.; Molina-Aldareguia, J.M.; Monclús, M.A.; González-Arrabal, R. Tribomechanical Properties of Hard Cr-Doped DLC Coatings Deposited by Low-Frequency HiPIMS. *Surf. Coat. Technol.* **2020**, *382*, 124899. [CrossRef]
5. Martins, P.S.; Pires, S.S.; da Silva, E.R.; Vieira, V.F.; Ba, E.C.T.; Dias, C.A.R. Tribological Aspects of the Diamond-like Carbon Film Applied to Different Surfaces of AISI M2 Steel. *Wear* **2022**, *506*, 204469. [CrossRef]
6. Yue, Z.; Fan, X.; Wang, Y.; Li, H.; Zhang, J.; Zhu, M. Fretting Behaviors of Self-Mated Diamond-like Carbon Films: The Evolution of Fretting Regime and Transfer Film. *Carbon N. Y.* **2023**, *203*, 695–705. [CrossRef]
7. Santhosh, N.; Shankar, G.; Nunthavarawong, P. Mechanical and Tribological Performance of Diamond-like Carbon Coatings: An Overview. *Diam.-Like Carbon Coat.* **2022**, 255–274.
8. Tasdemir, H.A.; Tokoroyama, T.; Kousaka, H.; Umehara, N.; Mabuchi, Y. Friction and Wear Performance of Boundary-Lubricated DLC/DLC Contacts in Synthetic Base Oil. *Procedia Eng.* **2013**, *68*, 518–524. [CrossRef]
9. Kumar, A.; Kumar, M.; Tailor, S. Self-Lubricating Composite Coatings: A Review of Deposition Techniques and Material Advancement. *Mater Today Proc.* **2023**. [CrossRef]
10. Zia, A.W.; Zhou, Z.; Li, L.K.-Y. Structural, Mechanical, and Tribological Characteristics of Diamond-like Carbon Coatings. In *Nanomaterials-Based Coatings*; Elsevier: Amsterdam, The Netherlands, 2019; pp. 171–194.
11. *ISO 20523:2017*; Carbon Based Films—Classification and Designations. The International Organization for Standardization, Vernier: Geneva, Switzerland, 2017.
12. Erdemir, A. Review of Engineered Tribological Interfaces for Improved Boundary Lubrication. *Tribol. Int.* **2005**, *38*, 249–256. [CrossRef]
13. Neville, A.; Morina, A.; Haque, T.; Voong, M. Compatibility between Tribological Surfaces and Lubricant Additives—How Friction and Wear Reduction Can Be Controlled by Surface/Lube Synergies. *Tribol. Int.* **2007**, *40*, 1680–1695. [CrossRef]
14. Velkavrh, I.; Kalin, M.; Vizintin, J. The Performance and Mechanisms of DLC-Coated Surfaces in Contact with Steel in Boundary-Lubrication Conditions: A Review. *Stroj. Vestn.* **2008**, *54*, 189–206.
15. Hsu, S.M.; Gates, R.S. Boundary Lubricating Films: Formation and Lubrication Mechanism. *Tribol. Int.* **2005**, *38*, 305–312. [CrossRef]
16. Suzuki, A.; Shinka, Y.; Masuko, M. Tribological Characteristics of Imidazolium-Based Room Temperature Ionic Liquids under High Vacuum. *Tribol. Lett.* **2007**, *27*, 307–313. [CrossRef]

17. Bermúdez, M.-D.; Jiménez, A.-E.; Sanes, J.; Carrión, F.-J. Ionic Liquids as Advanced Lubricant Fluids. *Molecules* **2009**, *14*, 2888–2908. [CrossRef]
18. Somers, A.E.; Khemchandani, B.; Howlett, P.C.; Sun, J.; MacFarlane, D.R.; Forsyth, M. Ionic Liquids as Antiwear Additives in Base Oils: Influence of Structure on Miscibility and Antiwear Performance for Steel on Aluminum. *ACS Appl. Mater. Interfaces* **2013**, *5*, 11544–11553. [CrossRef]
19. Zhou, Y.; Dyck, J.; Graham, T.W.; Luo, H.; Leonard, D.N.; Qu, J. Ionic Liquids Composed of Phosphonium Cations and Organophosphate, Carboxylate, and Sulfonate Anions as Lubricant Antiwear Additives. *Langmuir* **2014**, *30*, 13301–13311. [CrossRef]
20. Barnhill, W.C.; Qu, J.; Luo, H.; Meyer III, H.M.; Ma, C.; Chi, M.; Papke, B.L. Phosphonium-Organophosphate Ionic Liquids as Lubricant Additives: Effects of Cation Structure on Physicochemical and Tribological Characteristics. *ACS Appl. Mater. Interfaces* **2014**, *6*, 22585–22593. [CrossRef]
21. Barnhill, W.C.; Luo, H.; Meyer, H.M.; Ma, C.; Chi, M.; Papke, B.L.; Qu, J. Tertiary and Quaternary Ammonium-Phosphate Ionic Liquids as Lubricant Additives. *Tribol. Lett.* **2016**, *63*, 22. [CrossRef]
22. Minami, I.; Inada, T.; Sasaki, R.; Nanao, H. Tribo-Chemistry of Phosphonium-Derived Ionic Liquids. *Tribol. Lett.* **2010**, *40*, 225–235. [CrossRef]
23. Somers, A.E.; Biddulph, S.M.; Howlett, P.C.; Sun, J.; MacFarlane, D.R.; Forsyth, M. A Comparison of Phosphorus and Fluorine Containing IL Lubricants for Steel on Aluminium. *Phys. Chem. Chem. Phys.* **2012**, *14*, 8224–8231. [CrossRef] [PubMed]
24. Sharma, V.; Doerr, N.; Aswath, P.B. Chemical–Mechanical Properties of Tribofilms and Their Relationship to Ionic Liquid Chemistry. *RSC Adv.* **2016**, *6*, 22341–22356. [CrossRef]
25. Verma, D.K.; Dewangan, Y.; Singh, A.K.; Mishra, R.; Susan, M.A.B.H.; Salim, R.; Taleb, M.; El Hajjaji, F.; Berdimurodov, E. Ionic Liquids as Green and Smart Lubricant Application: An Overview. *Ionics* **2022**, *28*, 4923–4932. [CrossRef]
26. Wang, Y.-L.; Li, B.; Sarman, S.; Mocci, F.; Lu, Z.-Y.; Yuan, J.; Laaksonen, A.; Fayer, M.D. Microstructural and Dynamical Heterogeneities in Ionic Liquids. *Chem. Rev.* **2020**, *120*, 5798–5877. [CrossRef]
27. Groover, M.P. *Fundamentals of Modern Manufacturing: Materials, Processes, and Systems*; John Wiley & Sons: Hoboken, NJ, USA, 2020; ISBN 1119722012.
28. Tu, W.; Chat, K.; Szklarz, G.; Laskowski, L.; Grzybowska, K.; Paluch, M.; Richert, R.; Adrjanowicz, K. Dynamics of Pyrrolidinium-Based Ionic Liquids under Confinement. II. The Effects of Pore Size, Inner Surface, and Cationic Alkyl Chain Length. *J. Phys. Chem. C* **2019**, *124*, 5395–5408. [CrossRef]
29. Wang, Y.; Li, L. Uncovering the Underlying Mechanisms Governing the Solidlike Layering of Ionic Liquids (ILs) on Mica. *Langmuir* **2020**, *36*, 2743–2756. [CrossRef]
30. Kong, Q.; Zheng, S.S.; Liu, T.Q.; Nie, Y.; Song, K.D. Evaluation of Ionic Liquid "Greenness"-Cytotoxicity of Ionic Liquids. In Proceedings of the IOP Conference Series: Materials Science and Engineering, Wuhan, China, 10–12 October 2019; IOP Publishing: Bristol, UK, 2019; Volume 592, p. 012031.
31. Xiao, H.; Guo, D.; Liu, S.; Pan, G.; Lu, X. Film Thickness of Ionic Liquids under High Contact Pressures as a Function of Alkyl Chain Length. *Tribol. Lett.* **2011**, *41*, 471–477. [CrossRef]
32. Zhou, F.; Liang, Y.; Liu, W. Ionic Liquid Lubricants: Designed Chemistry for Engineering Applications. *Chem. Soc. Rev.* **2009**, *38*, 2590–2599. [CrossRef]
33. Jiménez, A.E.; Bermúdez, M.D.; Iglesias, P.; Carrión, F.J.; Martínez-Nicolás, G. 1-N-Alkyl-3-Methylimidazolium Ionic Liquids as Neat Lubricants and Lubricant Additives in Steel–Aluminium Contacts. *Wear* **2006**, *260*, 766–782. [CrossRef]
34. Qu, J.; Truhan, J.J.; Dai, S.; Luo, H.; Blau, P.J. Ionic Liquids with Ammonium Cations as Lubricants or Additives. *Tribol. Lett.* **2006**, *22*, 207–214. [CrossRef]
35. Minami, I.; Kita, M.; Kubo, T.; Nanao, H.; Mori, S. The Tribological Properties of Ionic Liquids Composed of Trifluorotris (Pentafluoroethyl) Phosphate as a Hydrophobic Anion. *Tribol. Lett.* **2008**, *30*, 215–223. [CrossRef]
36. Shah, F.U.; Glavatskih, S.; MacFarlane, D.R.; Somers, A.; Forsyth, M.; Antzutkin, O.N. Novel Halogen-Free Chelated Orthoborate–Phosphonium Ionic Liquids: Synthesis and Tribophysical Properties. *Phys. Chem. Chem. Phys.* **2011**, *13*, 12865–12873. [CrossRef] [PubMed]
37. Somers, A.E.; Howlett, P.C.; Sun, J.; MacFarlane, D.R.; Forsyth, M. Phosphonium Ionic Liquids as Lubricants for Aluminium-Steel. *Tribol. Des.* **2010**, *66*, 273–283.
38. Itoh, T.; Watanabe, N.; Inada, K.; Ishioka, A.; Hayase, S.; Kawatsura, M.; Minami, I.; Mori, S. Design of Alkyl Sulfate Ionic Liquids for Lubricants. *Chem. Lett.* **2009**, *38*, 64–65. [CrossRef]
39. Dupont, J.; Suarez, P.A.Z.; Umpierre, A.P.; de Souza, R.F. Pd (II)-Dissolved in Ionic Liquids: A Recyclable Catalytic System for the Selective Biphasic Hydrogenation of Dienes to Monoenes. *J. Braz. Chem. Soc.* **2000**, *11*, 293–297. [CrossRef]
40. Naveed, T.; Zahid, R.; Mufti, R.A.; Waqas, M.; Hanif, M.T. A Review on Tribological Performance of Ionic Liquids as Additives to Bio Lubricants. *Proc. Inst. Mech. Eng. Part J J. Eng. Tribol.* **2021**, *235*, 1782–1806. [CrossRef]
41. Jelínek, M.; Smetana, K.; Kocourek, T.; Dvořánková, B.; Zemek, J.; Remsa, J.; Luxbacher, T. Biocompatibility and Sp3/Sp2 Ratio of Laser Created DLC Films. *Mater. Sci. Eng. B* **2010**, *169*, 89–93. [CrossRef]
42. Jelínek, M.; Kocourek, T.; Remsa, J.; Mikšovský, J.; Zemek, J.; Smetana, K.; Dvořánková, B.; Luxbacher, T. Diamond/Graphite Content and Biocompatibility of DLC Films Fabricated by PLD. *Appl. Phys. A* **2010**, *101*, 579–583. [CrossRef]

43. Khanmohammadi, H.; Wijanarko, W.; Cruz, S.; Evaristo, M.; Espallargas, N. Triboelectrochemical Friction Control of W-and Ag-Doped DLC Coatings in Water–Glycol with Ionic Liquids as Lubricant Additives. *RSC Adv.* **2022**, *12*, 3573–3583. [CrossRef]
44. Qu, J.; Bansal, D.G.; Yu, B.; Howe, J.Y.; Luo, H.; Dai, S.; Li, H.; Blau, P.J.; Bunting, B.G.; Mordukhovich, G. Antiwear Performance and Mechanism of an Oil-Miscible Ionic Liquid as a Lubricant Additive. *ACS Appl. Mater. Interfaces* **2012**, *4*, 997–1002. [CrossRef]
45. Qu, J.; Luo, H.; Chi, M.; Ma, C.; Blau, P.J.; Dai, S.; Viola, M.B. Comparison of an Oil-Miscible Ionic Liquid and ZDDP as a Lubricant Anti-Wear Additive. *Tribol. Int.* **2014**, *71*, 88–97. [CrossRef]
46. Yu, B.; Bansal, D.G.; Qu, J.; Sun, X.; Luo, H.; Dai, S.; Blau, P.J.; Bunting, B.G.; Mordukhovich, G.; Smolenski, D.J. Oil-Miscible and Non-Corrosive Phosphonium-Based Ionic Liquids as Candidate Lubricant Additives. *Wear* **2012**, *289*, 58–64. [CrossRef]
47. Li, Z.; Dolocan, A.; Morales-Collazo, O.; Sadowski, J.T.; Celio, H.; Chrostowski, R.; Brennecke, J.F.; Mangolini, F. Lubrication Mechanism of Phosphonium Phosphate Ionic Liquid in Nanoscale Single-asperity Sliding Contacts. *Adv. Mater. Interfaces* **2020**, *7*, 2000426. [CrossRef]
48. Okubo, H.; Watanabe, S.; Tadokoro, C.; Sasaki, S. Effects of Concentration of Zinc Dialkyldithiophosphate on the Tribological Properties of Tetrahedral Amorphous Carbon Films in Presence of Organic Friction Modifiers. *Tribol. Int.* **2016**, *94*, 446–457. [CrossRef]
49. Okubo, H.; Watanabe, S.; Tadokoro, C.; Sasaki, S. Effects of Structure of Zinc Dialkyldithiophosphates on Tribological Properties of Tetrahedral Amorphous Carbon f Ilm under Boundary Lubrication. *Tribol. Int.* **2016**, *98*, 26–40. [CrossRef]
50. Okubo, H.; Tadokoro, C.; Sasaki, S. Tribological Properties of a Tetrahedral Amorphous Carbon (Ta-C) Film under Boundary Lubrication in the Presence of Organic Friction Modifiers and Zinc Dialkyldithiophosphate (ZDDP). *Wear* **2015**, *332*, 1293–1302. [CrossRef]
51. Kawada, S.; Watanabe, S.; Tadokoro, C.; Sasaki, S. Effects of Alkyl Chain Length of Sulfate and Phosphate Anion-Based Ionic Liquids on Tribochemical Reactions. *Tribol. Lett.* **2018**, *66*, 8. [CrossRef]
52. Kawada, S.; Watanabe, S.; Sasaki, S.; Miyatake, M. Tribochemical Reactions of Halogen-Free Ionic Liquids on Nascent Steel Surface. *Recent Adv. Ion. Liq. IntechOpen* **2018**, 47–65. [CrossRef]
53. Taokaew, S.; Kriangkrai, W. Recent Progress in Processing Cellulose Using Ionic Liquids as Solvents. *Polysaccharides* **2022**, *3*, 671–691. [CrossRef]
54. Hu, D.; Xiao, L.; Li, L.; Zhong, C.; Ju, X.; Yan, L.; Wu, T.; Qing, M.; Hu, Z. Effects of Ionic Liquid 1-Ethyl-3-Methylimidazolium Diethylphosphate on Cellulase Produced by Paenibacillus Sp. LLZ1. *ACS Sustain. Chem. Eng.* **2016**, *4*, 4922–4926. [CrossRef]
55. Dubey, S.; Bharmoria, P.; Gehlot, P.S.; Agrawal, V.; Kumar, A.; Mishra, S. 1-Ethyl-3-Methylimidazolium Diethylphosphate Based Extraction of Bioplastic "Polyhydroxyalkanoates" from Bacteria: Green and Sustainable Approach. *ACS Sustain. Chem. Eng.* **2018**, *6*, 766–773. [CrossRef]
56. Zeng, Q. Superlow Friction and Diffusion Behaviors of a Steel-Related System in the Presence of Nano Lubricant Additive in PFPE Oil. *J. Adhes Sci. Technol.* **2019**, *33*, 1001–1018. [CrossRef]
57. Forsberg, P.; Gustavsson, F.; Renman, V.; Hieke, A.; Jacobson, S. Performance of DLC Coatings in Heated Commercial Engine Oils. *Wear* **2013**, *304*, 211–222. [CrossRef]
58. Kosarieh, S.; Morina, A.; Lainé, E.; Flemming, J.; Neville, A. The Effect of MoDTC-Type Friction Modifier on the Wear Performance of a Hydrogenated DLC Coating. *Wear* **2013**, *302*, 890–898. [CrossRef]
59. Kalin, M.; Kogovšek, J.; Remškar, M. Nanoparticles as Novel Lubricating Additives in a Green, Physically Based Lubrication Technology for DLC Coatings. *Wear* **2013**, *303*, 480–485. [CrossRef]
60. Velkavrh, I.; Kalin, M. Effect of Base Oil Lubrication in Comparison with Non-Lubricated Sliding in Diamond-like Carbon Contacts. *Tribol.-Mater. Surf. Interfaces* **2011**, *5*, 53–58. [CrossRef]
61. Kalin, M.; Velkavrh, I.; Vižintin, J.; Ožbolt, L. Review of Boundary Lubrication Mechanisms of DLC Coatings Used in Mechanical Applications. *Meccanica* **2008**, *43*, 623–637. [CrossRef]
62. Kalin, M.; Velkavrh, I. Non-Conventional Inverse-Stribeck-Curve Behaviour and Other Characteristics of DLC Coatings in All Lubrication Regimes. *Wear* **2013**, *297*, 911–918. [CrossRef]
63. Balestra, R.M.; Castro, A.M.G.; Evaristo, M.; Escudeiro, A.; Mutafov, P.; Polcar, T.; Cavaleiro, A. Carbon-Based Coatings Doped by Copper: Tribological and Mechanical Behavior in Olive Oil Lubrication. *Surf. Coat. Technol.* **2011**, *205*, S79–S83. [CrossRef]
64. Manninen, N.K.; Ribeiro, F.; Escudeiro, A.; Polcar, T.; Carvalho, S.; Cavaleiro, A. Influence of Ag Content on Mechanical and Tribological Behavior of DLC Coatings. *Surf. Coat Technol.* **2013**, *232*, 440–446. [CrossRef]
65. Bociaga, D.; Komorowski, P.; Batory, D.; Szymanski, W.; Olejnik, A.; Jastrzebski, K.; Jakubowski, W. Silver-Doped Nanocomposite Carbon Coatings (Ag-DLC) for Biomedical Applications–Physiochemical and Biological Evaluation. *Appl. Surf. Sci.* **2015**, *355*, 388–397. [CrossRef]
66. Voevodin, A.A.; Capano, M.A.; Laube, S.J.P.; Donley, M.S.; Zabinski, J.S. Design of a Ti/TiC/DLC Functionally Gradient Coating Based on Studies of Structural Transitions in Ti–C Thin Films. *Thin. Solid Film.* **1997**, *298*, 107–115. [CrossRef]
67. Corbella, C.; Vives, M.; Pinyol, A.; Bertran, E.; Canal, C.; Polo, M.C.; Andújar, J.L. Preparation of Metal (W, Mo, Nb, Ti) Containing AC: H Films by Reactive Magnetron Sputtering. *Surf. Coat. Technol.* **2004**, *177*, 409–414. [CrossRef]
68. Zhao, F.; Li, H.; Ji, L.; Wang, Y.; Zhou, H.; Chen, J. Ti-DLC Films with Superior Friction Performance. *Diam Relat. Mater.* **2010**, *19*, 342–349. [CrossRef]
69. Evaristo, M.; Polcar, T.; Cavaleiro, A. Tribological Behaviour of W-alloyed Carbon-based Coatings in Dry and Lubricated Sliding Contact. *Lubr. Sci.* **2014**, *26*, 428–439. [CrossRef]

70. Ming, M.Y.; Jiang, X.; Piliptsou, D.G.; Zhuang, Y.; Rogachev, A.V.; Rudenkov, A.S.; Balmakou, A. Chromium-Modified AC Films with Advanced Structural, Mechanical and Corrosive-Resistant Characteristics. *Appl. Surf. Sci.* **2016**, *379*, 424–432. [CrossRef]
71. Wongpanya, P.; Silawong, P.; Photongkam, P. Adhesion and Corrosion of Al–N Doped Diamond-like Carbon Films Synthesized by Filtered Cathodic Vacuum Arc Deposition. *Ceram Int.* **2022**, *48*, 20743–20759. [CrossRef]
72. Fontes, M.A.; Serra, R.G.H.; Fernandes, F.D.; Cavaleiro Rodrigues de Carvalho, A.A.; Ferreira, F.E.d.S. Comparison of Mechanical and Tribological Properties of Diamond-like Carbon Coatings Doped with Europium and Gadolinium Produced by HiPIMS. *Proc. Inst. Mech. Eng. B J. Eng. Manuf.* **2022**, 09544054221136528. [CrossRef]
73. Omiya, T.; Fontes, M.; Vuchkov, T.; Cruz, S.; Cavaleiro, A.; Ferreira, F. Tribological Performance of Gd-DLC and Eu-DLC Coatings in the Presence of Synthetic Oils Containing Ionic Liquid Additives. *Tribol. Lett.* **2023**, *71*, 65. [CrossRef]
74. Sadeghi, M.; Omiya, T.; Fernandes, F.; Vilhena, L.; Ramalho, A.; Ferreira, F. Tribological Behavior of Doped DLC Coatings in the Presence of Ionic Liquid Additive under Different Lubrication Regimes. *Coatings* **2023**, *13*, 891. [CrossRef]
75. Valente, A.J.M.; Burrows, H.D.; Cruz, S.M.A.; Pereira, R.F.P.; Ribeiro, A.C.F.; Lobo, V.M.M. Aggregation and Micellization of Sodium Dodecyl Sulfate in the Presence of Ce (III) at Different Temperatures: A Conductometric Study. *J. Colloid Interface Sci.* **2008**, *323*, 141–145. [CrossRef] [PubMed]
76. Turanov, A.N.; Karandashev, V.K.; Boltoeva, M. Solvent Extraction of Intra-Lanthanides Using a Mixture of TBP and TODGA in Ionic Liquid. *Hydrometallurgy* **2020**, *195*, 105367. [CrossRef]
77. Mishra, B.B.; Niharbala, D. Application of Bifunctional Ionic Liquids for Extraction and Separation of Eu3+ from Chloride Medium. *Trans. Nonferrous Met. Soc. China* **2022**, *32*, 2061–2070. [CrossRef]
78. Stoy, L.; Xu, J.; Kulkarni, Y.; Huang, C.-H. Ionic Liquid Recovery of Rare-Earth Elements from Coal Fly Ash: Process Efficiency and Sustainability Evaluations. *ACS Sustain. Chem. Eng.* **2022**, *10*, 11824–11834. [CrossRef]
79. Rout, A.; Kumar, S.; Ramanathan, N. Probing the Coordination of Europium (III) in a Functionalized Ionic Liquid Using Luminescence Spectroscopy. *J. Mol. Liq.* **2021**, *323*, 115109. [CrossRef]
80. Yan, M.; Wang, X.; Zhang, S.; Zhang, S.; Sui, X.; Li, W.; Hao, J.; Liu, W. Friction and Wear Properties of GLC and DLC Coatings under Ionic Liquid Lubrication. *Tribol. Int.* **2020**, *143*, 106067. [CrossRef]
81. Bociąga, D.; Jakubowski, W.; Komorowski, P.; Sobczyk-Guzenda, A.; Jędrzejczak, A.; Batory, D.; Olejnik, A. Surface Characterization and Biological Evaluation of Silver-Incorporated DLC Coatings Fabricated by Hybrid RF PACVD/MS Method. *Mater. Sci. Eng. C* **2016**, *63*, 462–474. [CrossRef] [PubMed]
82. Najam-ul-Haq, M.; Rainer, M.; Huck, C.W.; Ashiq, M.N.; Bonn, G.K. Chemically Modified Diamond-like Carbon (DLC) for Protein Enrichment and Profiling by MALDI-MS. *Amino Acids* **2012**, *43*, 823–831. [CrossRef] [PubMed]
83. Chen, Z.; Ren, X.; Ren, L.; Wang, T.; Qi, X.; Yang, Y. Improving the Tribological Properties of Spark-Anodized Titanium by Magnetron Sputtered Diamond-like Carbon. *Coatings* **2018**, *8*, 83. [CrossRef]
84. Ze, S.; Dejun, K. Effect of Load on the Friction-Wear Behavior of Magnetron Sputtered DLC Film at High Temperature. *Mater. Res. Express* **2017**, *4*, 016404. [CrossRef]
85. Ghosh, S.; Choudhury, D.; Roy, T.; Mamat, A.B.; Masjuki, H.H.; Pingguan-Murphy, B. Tribological Investigation of Diamond-like Carbon Coated Micro-Dimpled Surface under Bovine Serum and Osteoarthritis Oriented Synovial Fluid. *Sci. Technol. Adv. Mater.* **2015**, *16*, 35002. [CrossRef] [PubMed]
86. Hatem, A.; Lin, J.; Wei, R.; Torres, R.D.; Laurindo, C.; Soares, P. Tribocorrosion Behavior of DLC-Coated Ti-6Al-4V Alloy Deposited by PIID and PEMS+ PIID Techniques for Biomedical Applications. *Surf. Coat. Technol.* **2017**, *332*, 223–232. [CrossRef]
87. Sharifahmadian, O.; Mahboubi, F.; Oskouie, A. Structural Evolution and Tribological Behavior of Nitrogen-Doped DLC Coatings Deposited by Pulsed DC PACVD Method. *Diam. Relat. Mater.* **2019**, *91*, 74–83. [CrossRef]
88. Lin, J.; Zhang, X.; Lee, P.; Wei, R. Thick Diamond like Carbon Coatings Deposited by Deep Oscillation Magnetron Sputtering. *Surf. Coat. Technol.* **2017**, *315*, 294–302. [CrossRef]
89. Hamrock, B.J.; Dowson, D. *Ball Bearing Lubrication: The Elastohydrodynamics of Elliptical Contacts*; NASA Lewis Research Center: Cleveland, OH, USA, 1981.
90. Hamrock, B.J.; Dowson, D. Isothermal Elastohydrodynamic Lubrication of Point Contacts: Part III—Fully Flooded Results. *J. Lubr. Technol.* **1977**, *99*, 264–275. [CrossRef]
91. Stachowiak, G.W.; Batchelor, A.W. *Engineering Tribology*; Butterworth-heinemann: Oxford, UK, 2013; ISBN 0123977762.
92. Tallian, T.E. On Competing Failure Modes in Rolling Contact. *ASLE Trans.* **1967**, *10*, 418–439. [CrossRef]
93. Balan, M.R.; Tufescu, A.; Cretu, S.S. A Case Study on Relation between Roughness, Lubrication and Fatigue Life of Rolling Bearings. In *Proceedings of the IOP Conference Series: Materials Science and Engineering*; IOP Publishing: Bristol, UK, 2016; Volume 147, p. 012013.
94. Harris, T.A.; Kotzalas, M.N. *Essential Concepts of Bearing Technology*; CRC Press: Boca Raton, FL, USA, 2006; ISBN 1420006592.
95. Mu, L.; Wu, J.; Matsakas, L.; Chen, M.; Vahidi, A.; Grahn, M.; Rova, U.; Christakopoulos, P.; Zhu, J.; Shi, Y. Lignin from Hardwood and Softwood Biomass as a Lubricating Additive to Ethylene Glycol. *Molecules* **2018**, *23*, 537. [CrossRef]
96. Song, J. Research Progress of Ionic Liquids as Lubricants. *ACS Omega* **2021**, *6*, 29345–29349. [CrossRef]
97. Yoshida, Y.; Baba, O.; Saito, G. Ionic Liquids Based on Dicyanamide Anion: Influence of Structural Variations in Cationic Structures on Ionic Conductivity. *J. Phys. Chem. B* **2007**, *111*, 4742–4749. [CrossRef]
98. Clarke, C.J.; Bui-Le, L.; Hallett, J.P.; Licence, P. Thermally-Stable Imidazolium Dicationic Ionic Liquids with Pyridine Functional Groups. *ACS Sustain. Chem. Eng.* **2020**, *8*, 8762–8772. [CrossRef]

99. Zorębski, E.; Musiał, M.; Dzida, M. Relation between Temperature–Pressure Dependence of Internal Pressure and Intermolecular Interactions in Ionic Liquids–Comparison with Molecular Liquids. *J. Chem. Thermodyn.* **2019**, *131*, 347–359. [CrossRef]
100. Ding, J.C.; Chen, M.; Mei, H.; Jeong, S.; Zheng, J.; Yang, Y.; Wang, Q.; Kim, K.H. Microstructure, Mechanical, and Wettability Properties of Al-Doped Diamond-like Films Deposited Using a Hybrid Deposition Technique: Bias Voltage Effects. *Diam. Relat. Mater.* **2022**, *123*, 108861. [CrossRef]
101. Evaristo, M.; Fernandes, F.; Cavaleiro, A. Room and High Temperature Tribological Behaviour of W-DLC Coatings Produced by DCMS and Hybrid DCMS-HiPIMS Configuration. *Coatings* **2020**, *10*, 319. [CrossRef]
102. Kasiorowski, T.; Lin, J.; Soares, P.; Lepienski, C.M.; Neitzke, C.A.; De Souza, G.B.; Torres, R.D. Microstructural and Tribological Characterization of DLC Coatings Deposited by Plasma Enhanced Techniques on Steel Substrates. *Surf. Coat. Technol.* **2020**, *389*, 125615. [CrossRef]
103. Aijaz, A.; Ferreira, F.; Oliveira, J.; Kubart, T. Mechanical Properties of Hydrogen Free Diamond-like Carbon Thin Films Deposited by High Power Impulse Magnetron Sputtering with Ne. *Coatings* **2018**, *8*, 385. [CrossRef]
104. Yetim, A.F.; Kovacı, H.; Kasapoğlu, A.E.; Bozkurt, Y.B.; Çelik, A. Influences of Ti, Al and V Metal Doping on the Structural, Mechanical and Tribological Properties of DLC Films. *Diam. Relat. Mater.* **2021**, *120*, 108639. [CrossRef]
105. Bai, M.; Yang, L.; Li, J.; Luo, L.; Sun, S.; Inkson, B. Mechanical and Tribological Properties of Si and W Doped Diamond like Carbon (DLC) under Dry Reciprocating Sliding Conditions. *Wear* **2021**, *484*, 204046. [CrossRef]
106. Wang, Q.J.; Chung, Y.-W. *Encyclopedia of Tribology: With 3650 Figures and 493 Tables*; Springer: Berlin/Heidelberg, Germany, 2013; ISBN 0387928979.
107. Marinescu, I.D.; Rowe, W.B.; Dimitrov, B.; Inaski, I. *Tribology of Abrasive Machining Processes*; Elsevier: Amsterdam, The Netherlands, 2004; ISBN 0815519389.
108. Li, P.; Zhang, F.; Zhang, H.; Wang, T.; Wang, Q.; Qiao, W. Lubrication Performance of Kite-Shaped Microtexture under Hydrodynamic Lubrication. *Tribol. Int.* **2023**, *179*, 108144. [CrossRef]
109. Kalin, M.; Velkavrh, I.; Vižintin, J. The Stribeck Curve and Lubrication Design for Non-Fully Wetted Surfaces. *Wear* **2009**, *267*, 1232–1240. [CrossRef]
110. Linjamaa, A.; Lehtovaara, A.; Kallio, M.; Léger, A. Running-in Effects on Friction of Journal Bearings under Slow Sliding Speeds. *Proc. Inst. Mech. Eng. Part J J. Eng. Tribol.* **2020**, *234*, 362–372. [CrossRef]
111. Xin, Q. Friction and Lubrication in Diesel Engine System Design. *Diesel Engine Syst. Des.* **2013**, *1*, 651–758.
112. Martini, A.; Zhu, D.; Wang, Q. Friction Reduction in Mixed Lubrication. *Tribol. Lett.* **2007**, *28*, 139–147. [CrossRef]
113. Wang, Y.; Wang, Q.J.; Lin, C.; Shi, F. Development of a Set of Stribeck Curves for Conformal Contacts of Rough Surfaces. *Tribol. Trans.* **2006**, *49*, 526–535. [CrossRef]
114. Lu, X.; Khonsari, M.M.; Gelinck, E.R.M. The Stribeck Curve: Experimental Results and Theoretical Prediction. *J. Tribol.* **2006**, *128*, 789–794. [CrossRef]
115. Xiao, H. Ionic Liquid Lubricants: Basics and Applications. *Tribol. Trans.* **2017**, *60*, 20–30. [CrossRef]
116. Kajdas, C. Importance of Anionic Reactive Intermediates for Lubricant Component Reactions with Friction Surfaces. *Lubr. Sci.* **1994**, *6*, 203–228. [CrossRef]
117. Perkin, S.; Albrecht, T.; Klein, J. Layering and Shear Properties of an Ionic Liquid, 1-Ethyl-3-Methylimidazolium Ethylsulfate, Confined to Nano-Films between Mica Surfaces. *Phys. Chem. Chem. Phys.* **2010**, *12*, 1243–1247. [CrossRef] [PubMed]
118. Atkin, R.; El Abedin, S.Z.; Hayes, R.; Gasparotto, L.H.S.; Borisenko, N.; Endres, F. AFM and STM Studies on the Surface Interaction of [BMP] TFSA and [EMIm] TFSA Ionic Liquids with Au (111). *J. Phys. Chem. C* **2009**, *113*, 13266–13272. [CrossRef]